

AM concentrations than those with more active variants of this enzyme. However, because DHA also has an antimalarial effect, it would be difficult to assess the clinical outcome in subjects who polymorphically express CYP2B6 without *in vivo* data. To more fully understand the mechanistic basis of our findings, it would be of great value to clinically examine the relationship between CYP2B6 genotypes and the plasma concentration of AM and its metabolites.

In conclusion, demethylation of AM was mainly catalyzed by recombinant CYP2B6, although recombinant CYP3A4 also exhibited this metabolic activity. In addition, we performed a comprehensive analysis, using COS-7 cells as a heterologous expression system, to characterize nonsynonymous CYP2B6 variants. Many of the 26 variants expressed in COS-7 cells exhibited significantly altered AM demethylation activity. This study provides insights into the genotype-phenotype associations of CYP2B6 and lays a foundation for future clinical studies on interindividual variation in drug efficacy and toxicity.

Authorship Contributions

Participated in research design: Honda, Hirasawa, and Hiratsuka.

Conducted experiments: Honda, Muroi, and Tamaki.

Contributed new reagents or analytic tools: Saigusa, Suzuki, Tomioka, and Matsubara.

Performed data analysis: Honda, Oda, and Hiratsuka.

Wrote or contributed to the writing of the manuscript: Honda, Saigusa, and Hiratsuka.

References

- Ali S, Najmi MH, Tarning J, and Lindegardh N (2010) Pharmacokinetics of artemether and dihydroartemisinin in healthy Pakistani male volunteers treated with artemether-lumefantrine. *Malar J* **9**:275.
- Arenaz I, Vicente J, Fanlo A, Vázquez P, Medina JC, Conde B, González-Andrade F, and Sinués B (2010) Haplotype structure and allele frequencies of CYP2B6 in Spaniards and Central Americans. *Fundam Clin Pharmacol* **24**:247–253.
- Asimus S and Ashton M (2009) Artemisinin—a possible CYP2B6 probe substrate? *Biopharm Drug Dispos* **30**:265–275.
- Brewer TG, Grate SJ, Peggins JO, Weina PJ, Petras JM, Levine BS, Heiffer MH, and Schuster BG (1994) Fetal neurotoxicity of artemether and artemether. *Am J Trop Med Hyg* **51**:251–259.
- Gautam A, Ahmed T, Batra V, and Palival J (2009) Pharmacokinetics and pharmacodynamics of endoperoxide antimalarials. *Curr Drug Metab* **10**:289–306.
- Gay SC, Shah MB, Talakad JC, Maekawa K, Roberts AG, Wilderman PR, Sun L, Yang JY, Huelga SC, Hong WX, et al. (2010) Crystal structure of a cytochrome P450 2B6 genetic variant in complex with the inhibitor 4-(4-chlorophenyl)imidazole at 2.0-Å resolution. *Mol Pharmacol* **77**:529–538.
- Hesse LM, Venkatakrishnan K, Court MH, von Moltke LL, Duan SX, Shader RI, and Greenblatt DJ (2000) CYP2B6 mediates the *in vitro* hydroxylation of bupropion: potential drug interactions with other antidepressants. *Drug Metab Dispos* **28**:1176–1183.
- Hidestrand M, Oscarson M, Salonen JS, Nyman L, Pelkonen O, Turpeinen M, and Ingelman-Sundberg M (2001) CYP2B6 and CYP2C19 as the major enzymes responsible for the metabolism of selegiline, a drug used in the treatment of Parkinson's disease, as revealed from experiments with recombinant enzymes. *Drug Metab Dispos* **29**:1480–1484.
- Hien TT and White NJ (1993) Qinghaosu. *Lancet* **341**:603–608.
- Human Cytochrome P450 (CYP) Allele Nomenclature Committee (2008) CYP2B6 nomenclature. Available at: <http://www.cypalleles.ki.se/cyp2b6.htm>.
- Huang L, Jayewardene AL, Li X, Marzan F, Lizak PS, and Aweeka FT (2009) Development and validation of a high-performance liquid chromatography/tandem mass spectrometry method for the determination of artemether and its active metabolite dihydroartemisinin in human plasma. *J Pharm Biomed Anal* **50**:959–965.
- Jinno H, Tanaka-Kagawa T, Ohno A, Makino Y, Matsushima E, Hanioka N, and Ando M (2003) Functional characterization of cytochrome P450 2B6 allelic variants. *Drug Metab Dispos* **31**:398–403.
- Klayman DL (1985) Qinghaosu (artemisinin): an antimalarial drug from China. *Science* **228**:1049–1055.
- Klein K, Lang T, Saussele T, Barbosa-Sicard E, Schunck WH, Eichelbaum M, Schwab M, and Zanger UM (2005) Genetic variability of CYP2B6 in populations of African and Asian origin: allele frequencies, novel functional variants, and possible implications for anti-HIV therapy with efavirenz. *Pharmacogenet Genomics* **15**:861–873.
- Lang T, Klein K, Richter T, Zibat A, Kerb R, Eichelbaum M, Schwab M, and Zanger UM (2004) Multiple novel nonsynonymous CYP2B6 gene polymorphisms in Caucasians: demonstration of phenotypic null alleles. *J Pharmacol Exp Ther* **311**:34–43.
- Le Bras J and Durand R (2003) The mechanisms of resistance to antimalarial drugs in *Plasmodium falciparum*. *Fundam Clin Pharmacol* **17**:147–153.
- Lefèvre G, Carpenter P, Souppart C, Schmidli H, McClean M, and Stypinski D (2002) Pharmacokinetics and electrocardiographic pharmacodynamics of artemether-lumefantrine (Riamet) with concomitant administration of ketoconazole in healthy subjects. *Br J Clin Pharmacol* **54**:485–492.
- Mo SL, Liu YH, Duan W, Wei MQ, Kanwar JR, and Zhou SF (2009) Substrate specificity, regulation, and polymorphism of human cytochrome P450 2B6. *Curr Drug Metab* **10**:730–753.
- Mordi MN, Mansor SM, Navaratnam V, and Wernsdorfer WH (1997) Single dose pharmacokinetics of oral artemether in healthy Malaysian volunteers. *Br J Clin Pharmacol* **43**:363–365.
- Mwesigwa J, Parikh S, McGee B, German P, Drysdale T, Kalyango JN, Clark TD, Dorsey G, Lindegardh N, Annerberg A, et al. (2010) Pharmacokinetics of artemether-lumefantrine and artesunate-amodiaquine in children in Kampala, Uganda. *Antimicrob Agents Chemother* **54**:52–59.
- Na Bangchang K, Karbwang J, Thomas CG, Thanavibul A, Sukontason K, Ward SA, and Edwards G (1994) Pharmacokinetics of artemether after oral administration to healthy Thai males and patients with acute, uncomplicated falciparum malaria. *Br J Clin Pharmacol* **37**:249–253.
- Nakajima M, Komagata S, Fujiki Y, Kanada Y, Ebi H, Itoh K, Mukai H, Yokoi T, and Minami H (2007) Genetic polymorphisms of CYP2B6 affect the pharmacokinetics/pharmacodynamics of cyclophosphamide in Japanese cancer patients. *Pharmacogenet Genomics* **17**:431–445.
- Navaratnam V, Mansor SM, Sit NW, Grace J, Li Q, and Olliaro P (2000) Pharmacokinetics of artemisinin-type compounds. *Clin Pharmacokinet* **39**:255–270.
- Price RN and Nosten F (2001) Drug resistant falciparum malaria: clinical consequences and strategies for prevention. *Drug Resist Updat* **4**:187–196.
- Rotger M, Tegude H, Colombo S, Cavassini M, Furrer H, Décosterd L, Bliedernicht J, Saussele T, Günthard HF, Schwab M, et al. (2007) Predictive value of known and novel alleles of CYP2B6 for efavirenz plasma concentrations in HIV-infected individuals. *Clin Pharmacol Ther* **81**:557–566.
- Roy P, Yu LJ, Crespi CL, and Waxman DJ (1999) Development of a substrate-activity based approach to identify the major human liver P-450 catalysts of cyclophosphamide and ifosfamide activation based on cDNA-expressed activities and liver microsomal P-450 profiles. *Drug Metab Dispos* **27**:655–666.
- Salonen JS, Nyman L, Boobis AR, Edwards RJ, Watts P, Lake BG, Price RJ, Renwick AB, Gómez-Lechón MJ, Castell JV, et al. (2003) Comparative studies on the cytochrome p450-associated metabolism and interaction potential of selegiline between human liver-derived *in vitro* systems. *Drug Metab Dispos* **31**:1093–1102.
- van Agtmael MA, Cheng-Qi S, Qing JX, Mull R, and van Bostel CJ (1999a) Multiple dose pharmacokinetics of artemether in Chinese patients with uncomplicated falciparum malaria. *Int J Antimicrob Agents* **12**:151–158.
- van Agtmael MA, Gupta V, van der Graaf CA, and van Bostel CJ (1999b) The effect of grapefruit juice on the time-dependent decline of artemether plasma levels in healthy subjects. *Clin Pharmacol Ther* **66**:408–414.
- van Agtmael MA, Gupta V, van der Wösten TH, Rutten JP, and van Bostel CJ (1999c) Grapefruit juice increases the bioavailability of artemether. *Eur J Clin Pharmacol* **55**:405–410.
- van Agtmael MA, Van Der Graaf CA, Dien TK, Koopmans RP, and van Bostel CJ (1998) The contribution of the enzymes CYP2D6 and CYP2C19 in the demethylation of artemether in healthy subjects. *Eur J Drug Metab Pharmacokinet* **23**:429–436.
- Wang J, Sönnnerborg A, Rane A, Josephson F, Lundgren S, Ståhle L, and Ingelman-Sundberg M (2006) Identification of a novel specific CYP2B6 allele in Africans causing impaired metabolism of the HIV drug efavirenz. *Pharmacogenet Genomics* **16**:191–198.
- Watanabe T, Sakuyama K, Sasaki T, Ishii Y, Ishikawa M, Hirasawa N, and Hiratsuka M (2010) Functional characterization of 26 CYP2B6 allelic variants (CYP2B6.2–CYP2B6.28, except CYP2B6.22). *Pharmacogenet Genomics* **20**:459–462.
- Wernsdorfer WH (1991) The development and spread of drug-resistant malaria. *Parasitol Today* **7**:297–303.
- Woodrow CJ, Haynes RK, and Krishna S (2005) *Artemisinins Postgrad Med J* **81**:71–78.
- World Health Organization (2010) *Guidelines for Treatment of Malaria*, 2nd ed., World Health Organization, Geneva, Switzerland. Available from http://whqlibdoc.who.int/publications/2010/9789241547925_eng.pdf.
- Xie H, Griskevicius L, Ståhle L, Hassan Z, Yasar U, Rane A, Broberg U, Kimby E, and Hassan M (2006) Pharmacogenetics of cyclophosphamide in patients with hematological malignancies. *Eur J Pharm Sci* **27**:54–61.
- Xie HJ, Yasar U, Lundgren S, Griskevicius L, Terelius Y, Hassan M, and Rane A (2003) Role of polymorphic human CYP2B6 in cyclophosphamide bioactivation. *Pharmacogenomics J* **3**:53–61.
- Zanger UM, Klein K, Saussele T, Bliedernicht J, Hofmann MH, and Schwab M (2007) Polymorphic CYP2B6: molecular mechanisms and emerging clinical significance. *Pharmacogenomics* **8**:743–759.

Address correspondence to: Dr. Masahiro Hiratsuka, Laboratory of Pharmacotherapy of Life-Style Related Diseases, Graduate School of Pharmaceutical Sciences, Tohoku University, Sendai, Japan, 6-3, Aoba, Aramaki, Aoba-ku, Sendai 980-8578, Japan. E-mail: mhira@m.tohoku.ac.jp

Selective inhibition of EGFR and VEGFR2 tyrosine kinases controlled by a boronic acid substituent on 4-anilinoquinazolines†

Hiroyuki Nakamura,* Ryoji Horikoshi, Taikou Usui and Hyun Seung Ban

Received 20th July 2010, Accepted 13th August 2010

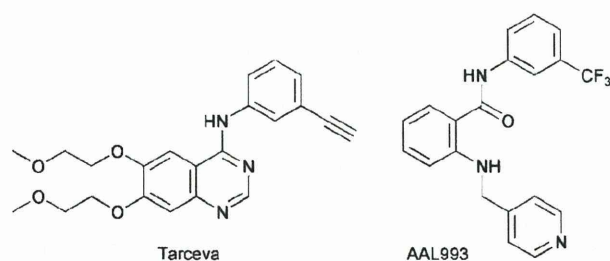
DOI: 10.1039/c0md000115e

Boronic acid-containing 4-anilinoquinazolines were synthesized as selective inhibitors of EGFR and VEGFR2 tyrosine kinases. The substituted position of the boronic acid is essential for control of both kinase inhibitions, and the boronic acid substituted at the *para* position of the aniline moiety exhibited significant inhibition of VEGFR2 tyrosine kinase.

Growth factor receptor tyrosine kinases play an important role for the signal transduction pathway in cell proliferation. Deregulation of the signaling pathway has been observed in many human tumors, thus these kinases have been investigated as potential targets for cancer therapy.¹ The kinase inhibitors competitively bind to the ATP binding site of the protein kinases, which is relatively conserved, therefore enzymatic selectivity has been required for development of the kinase inhibitors. Among the various protein tyrosine kinase inhibitors reported,² the 4-anilinoquinazolines have proved to have great potential for selectivity and potency.³ In 1994, Fry and coworkers first found the 4-anilinoquinazoline (PD153035) to be a specific inhibitor of epidermal growth factor receptor (EGFR) tyrosine kinase.⁴ Based on their findings, ZD-1839 (Iressa™)^{5,6} and OSI-774 (Tarceva™)^{7,8} have been developed as EGFR tyrosine kinase inhibitors and approved for non-small cell lung cancer (NSCLC) therapy. In the meantime, various 4-anilinoquinazoline framework-based protein kinase inhibitors have been reported including cyclin-dependent kinase 2 (CDK2),⁹ Src and Abl kinases,¹⁰ vascular endothelial growth factor receptor (VEGFR) tyrosine kinases,¹¹ and platelet-derived growth factor receptor (PDGFR) kinase.¹²

between the neutral sp² and the anionic sp³ hybridization states, which generates a new stable interaction between a boron atom and a donor molecule through a covalent bond. In particular, several boronic acid compounds have been studied as enzyme inhibitors including thrombin,¹⁴ lactamases,¹⁵ dipeptidyl peptidases,¹⁶ and others.^{17–20} However, the most promising achievement in the area of boron pharmaceuticals is the development of bortezomib (PS341), a proteasome inhibitor,²¹ recently approved for clinical treatment of relapsed multiple myeloma and mantle cell lymphoma. The X-ray crystal structure of the 20S proteasome in complex with bortezomib was reported. In this structure, the boronic acid of bortezomib covalently interacts with the Thr-1 hydroxyl in the active site of the 20S proteasome, forming the hybridized borate.²² Recently, we reported the prolonged inhibitory activity of a boron-conjugated 4-anilinoquinazoline toward the EGFR tyrosine kinase. The quantum mechanical docking simulation revealed that the boronic acid moiety substituted at the 6 position of the quinazoline with a benzyl linker formed a covalent B–O bond with Asp800 in addition to hydrogen bonds with Asp800 and Cys797, which may cause the prolonged inhibition of the compound toward EGFR tyrosine kinase.²³ In this paper, we introduce a boronic acid, as an alternative candidate for a functional group, into the 4-anilinoquinazoline framework in pharmaceutical drug design and found that the selective inhibition of EGFR and VEGFR tyrosine kinases was controlled by a boronic acid substituent on 4-anilinoquinazolines (Fig. 1).

The synthesis of the diboron coupling precursors **3** and **5** is shown in Scheme 1. Substitution of 4-chloroquinazoline **1** with 3-chloroaniline and 3-chloro-4-fluoroaniline gave the corresponding 4-anilinoquinazolines **3a** and **3b** in 69 and 87% yields, respectively.²⁴ In a similar manner, 4-chloroquinazoline **2** was reacted with 3-chloroaniline and 3-chloro-4-fluoroaniline, and the resulting 4-anilinoquinazolines **4a** and **4b** were treated with aqueous ammonia followed by anhydrous trifluoromethane



Although organoborons have been developed as nucleophilic reagents for C–C bond formation in organic synthesis,¹³ the use of boron as a candidate functional group to interact with a target protein is an attractive strategy for drug design in medicine. A boron atom has a vacant orbital and interconverts with ease

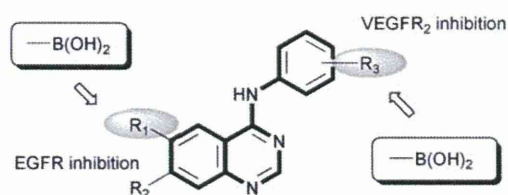
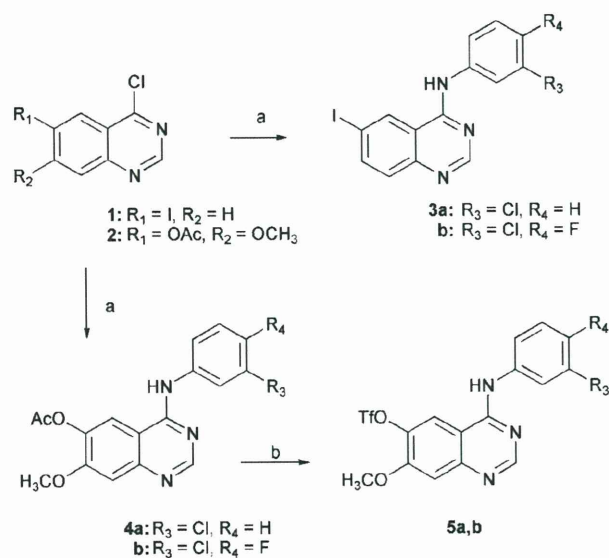


Fig. 1 Design of boronic acid-containing 4-anilinoquinazolines.

Department of Chemistry, Faculty of Science, Gakushuin University, Mejiro, Toshima-ku, Tokyo 171-8588, Japan. E-mail: hiroyuki.nakamura@gakushuin.ac.jp; Fax: +81 3 3986 0221; Tel: +81 3 5992 1029 † Electronic supplementary information (ESI) available: Experimental procedures and full characterisation for all new compounds. See DOI: 10.1039/c0md000115e

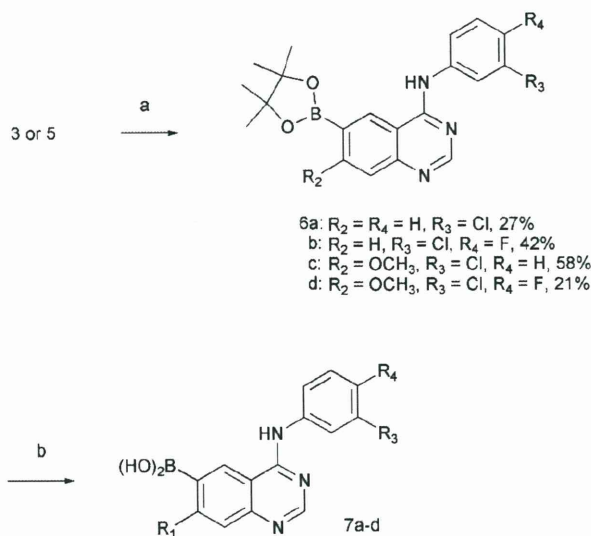


Scheme 1 Reagents and conditions: (a) anilines, isopropanol, reflux, **3a** (69%) or **3b** (87%); (b) i) 25% NH_3 aq; ii) Tf_2O , Py.

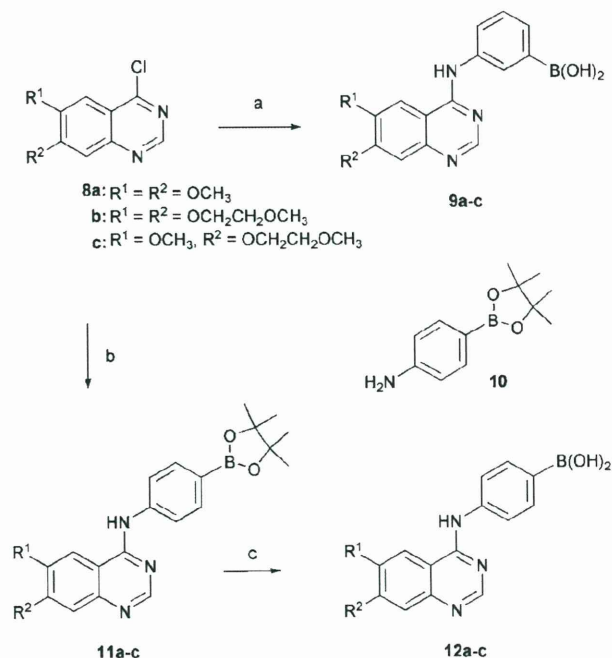
sulfonic acid to afford the corresponding triflates **5a** and **5b** in 15 and 66% yields, respectively, from **2** in three steps.

The Suzuki–Miyaura diboron coupling reaction was employed for **3** or **5** in the presence of palladium(II) catalysts in dimethylformamide (DMF) at 80 °C to give **6a–d** in 21–58% yields. Finally, deprotection of the pinacol boronate moiety was carried out under transesterification conditions using KHF_2 and phenylboronic acid to afford the corresponding boronic acids **7a–d** in 32–48% yields (Scheme 2).

Meanwhile, the boron-conjugated 4-anilinoquinazolines, in which a boronic acid moiety was substituted on the aniline ring, were synthesized by the substitution reaction of chloroquinazolines **8a–c** and boronated anilines as shown in Scheme 3. The



Scheme 2 Reagents and conditions: (a) pinacolodiboron, PdCl_2 , dppf, KOAc, DMF, 80 °C; (b) i) KHF_2 , $\text{MeOH-H}_2\text{O}$; ii) $\text{PhB}(\text{OH})_2$.



Scheme 3 Reagents and conditions: (a) i) (3-aminophenyl)boronic acid, conc. HCl, isopropanol; ii) NaHCO_3 , $\text{MeOH-H}_2\text{O}$; (b) **10**, conc. HCl, isopropanol; (c) KHF_2 , $\text{MeOH-H}_2\text{O}$.

m-substituted boronic acids **9a–c** were obtained from **8a–c** with (3-aminophenyl)boronic acid under acidic conditions. On the contrary, the *p*-substituted boronic acids **12a–c** were obtained from **8a–c** with commercially available pinacolboronic ester **10** under acidic condition. The resulting boronic esters **11a–c** were treated with KHF_2 to afford the corresponding boronic acids **12a–c**.

Inhibitory activity of the boron-conjugated 4-anilinoquinazolines **6**, **7**, **9** and **12** against EGFR, HER2, Flt-1 and KDR tyrosine kinases was determined by measuring the levels of phosphorylation of the tyrosine kinase-specific peptides (poly-(Glu:Tyr) substrate) *in vitro*.²⁵ As shown in Table 1, the boron-conjugated 4-anilinoquinazolines **6a–d** and **7a–d**, which have a boronate ester or boronic acid group substituted at the C-6 position of the quinazoline framework, selectively suppressed EGFR tyrosine kinase activity without inhibiting HER2, Flt-1 (VEGFR1 tyrosine kinase catalytic domain) or KDR (VEGFR2 tyrosine kinase catalytic domain) kinases, and their IC_{50} values against EGFR tyrosine kinase were at the range of 0.46–0.80 μM . On the contrary, the compounds **9a–c**, and **12a–c**, which have a boronic acid group substituted at the aniline ring of the quinazolines, displayed selective inhibition toward KDR tyrosine kinase. In particular, a boronic acid group substituted at the *para* position of the aniline, such as the compounds **12a–c**, is potent for significant inhibitory activity of KDR. The IC_{50} values of **12a** and **12b** are 0.036 and 0.037 μM , respectively, which is similar to that of a known KDR inhibitor, AAL993 ($\text{IC}_{50} = 0.014 \mu\text{M}$).²⁶

We next examined the effects of the boron-conjugated 4-anilinoquinazolines on the EGF-induced tyrosine phosphorylation of EGFR and the signaling cascades in A431 cells by immunoblot analysis. Treatment of A431 with EGF (10 ng ml^{-1}) rapidly

Table 1 Effect of the boron-conjugated 4-anilinoquinazolines on tyrosine kinase activity of EGFR, HER2, Flt-1, and KDR

Compds	IC ₅₀ /μM ^a			
	EGFR	HER2 ^b	Flt-1 ^b	KDR ^b
6a	0.59 ± 0.03	>1 (31)	>1 (12)	>1 (-)
6b	0.57 ± 0.04	>1 (-)	>1 (8)	>1 (-)
6c	0.49 ± 0.08	>1 (-)	>1 (-)	>1 (-)
6d	0.52 ± 0.07	>1 (-)	>1 (-)	>1 (-)
7a	0.65 ± 0.02	>1 (15)	>1 (7)	>1 (-)
7b	0.80 ± 0.07	>1 (-)	>1 (-)	>1 (-)
7c	0.46 ± 0.05	>1 (-)	>1 (-)	>1 (-)
7d	0.51 ± 0.01	>1 (-)	>1 (-)	>1 (-)
9a	>1 (46)	>1 (-)	>1 (-)	0.39 ± 0.03
9b	>1 (24)	>1 (-)	>1 (-)	0.19 ± 0.02
9c	>1 (45)	>1 (-)	>1 (19)	0.18 ± 0.02
12a	>1 (40)	>1 (-)	>1 (49)	0.036 ± 0.006
12b	>1 (36)	>1 (-)	>1 (41)	0.037 ± 0.012
12c	>1 (28)	>1 (-)	>1 (-)	0.86 ± 0.12
Tarceva	0.047 ± 0.003	>1 (-)	>1 (-)	>1 (38)
AAL993	>1 (30)	>1 (-)	>1 (-)	0.014 ± 0.002

^a The drug concentrations required to inhibit the phosphorylation of the poly(Glu:Tyr) substrate by 50% (IC₅₀) were determined from semilogarithmic dose-response plots, and results represent mean ± s.d. of triplicate samples. Percent of inhibition at 1 μM concentration was indicated in parentheses. ^b -, no inhibitory effect at 1 μM.

induced autophosphorylation of EGFR, and the level of the phosphorylation reached a maximum at 10 min after EGF stimulation. Under these conditions, the boron-conjugated 4-anilinoquinazolines, **6a-d** and **7a-d**, potently suppressed the EGF-induced phosphorylation of EGFR at 1 μM concentration

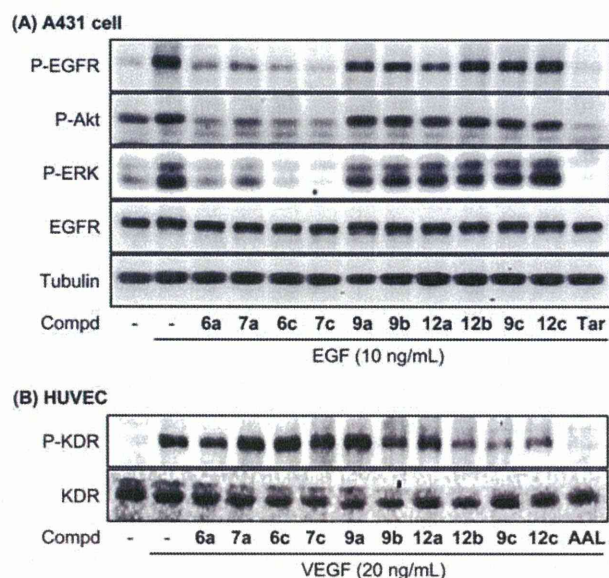
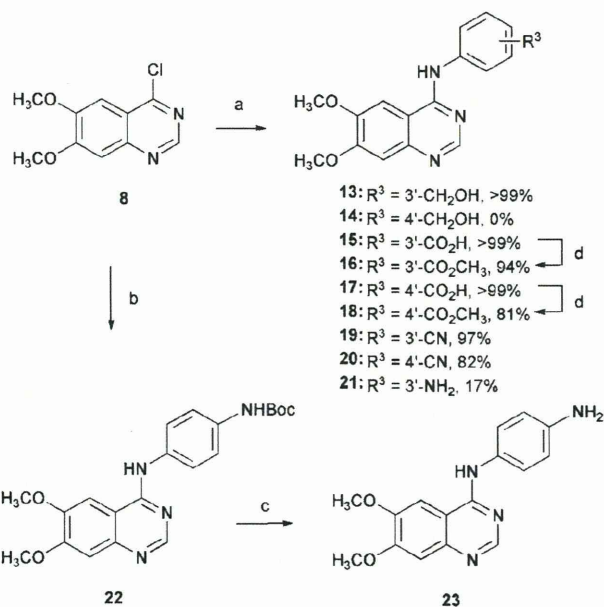


Fig. 2 Inhibition of the EGF-induced phosphorylation of EGFR and VEGF-induced phosphorylation of KDR. (A) A431 cells were incubated with the boron-conjugated 4-anilinoquinazolines (1 μM) or Tarceva (0.3 μM) and then stimulated with EGF (10 ng mL⁻¹). (B) HUVECs were incubated with the boron-conjugated 4-anilinoquinazolines (1 μM) or AAL993 (1 μM) and then stimulated with VEGF (20 ng mL⁻¹). The levels of each kinase were detected by immunoblot analysis with the specific antibody.



Scheme 4 Reagents and conditions: (a) anilines, isopropanol, reflux; (b) 4-(BocNH)C₆H₄NH₂, isopropanol, reflux, 87%; (c) TFA, CH₂Cl₂, >99%; (d) conc. HCl, CH₃OH.

of compounds, whereas compounds **9a-c** and **12a-c** did not affect the EGFR phosphorylation at this concentration (Fig. 2A). It has been reported that the autophosphorylation of EGFR tyrosine kinase activated various downstream kinases including ERK and Akt, which play an important role in the regulation of cell proliferation and apoptosis, respectively.²⁷ Therefore, we examined the effects on the EGFR-dependent activation of downstream signaling pathways. The boron-conjugated 4-anilinoquinazolines, **6a-d** and **7a-d**, also significantly suppressed the EGF-induced phosphorylation of ERK and Akt in parallel with the inhibition of EGFR autophosphorylation. However, these inhibitions were not observed in compounds **9a-c** and **12a-c**. These results indicate that the boron-conjugated 4-anilinoquinazolines, **6a-d** and **7a-d**, also induce the inhibitory effect on autophosphorylation of EGFR tyrosine kinase in cells as well as EGFR kinase *in vitro*, and arrest the downstream signaling pathway. Furthermore, we examined the effects of the boron-conjugated 4-anilinoquinazolines on the VEGF-induced phosphorylation of KDR in HUVECs. As shown in Fig. 2B, boron-conjugated 4-anilinoquinazolines **9b**, **9c**, **12b** and **12c** significantly suppressed VEGF-induced KDR phosphorylation. Although compounds **9a** and **12a** potentially inhibited KDR kinase activity (Table 1), their inhibitory effect on KDR phosphorylation in HUVECs was not observed. The discrepancy of results between kinase assay and immunoblotting analysis might be induced by the weak membrane permeability property of dimethoxy groups in compounds **9a** and **12a**.

Since the substitution of a boronic acid group on the aniline ring has been observed to be essential for selective inhibition of KDR tyrosine kinase, we next synthesized various functional groups-substituted 4-anilinoquinazolines from 4-chloroquinazolinone **8** and anilines, and examined their effects on tyrosine kinase activity of EGFR, HER2, Flt-1, and KDR. As shown in

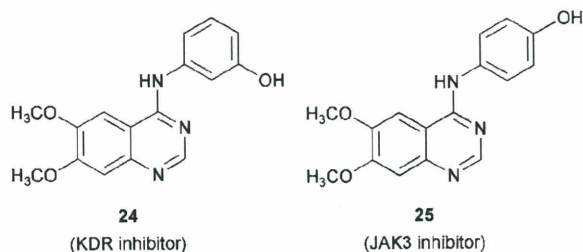
Table 2 Inhibition of the Various Functional Groups-Substituted 4-Anilinoquinazolines on Tyrosine Kinase Activity of EGFR, HER2, Flt-1, and KDR at 1 μ M Concentration

Comps	% Inhibition at 1 μ M ^a			
	EGFR ^b	HER2 ^b	Flt-1 ^b	KDR ^b
12a	40	—	49	99
12b	36	—	41	99
13	35	—	—	11
15	—	—	32	7
16	16	—	—	23
17	7	—	—	6
18	10	—	—	21
19	80	—	—	9
20	5	—	—	—
21	52	—	—	8
23	27	5	—	4
24	72	57	32	88
25	59	—	—	31
Tarceva	82	—	—	38
AAL993	30	—	34	95

^a Percent of inhibition of the phosphorylation of the poly(Glu:Ty) substrate at 1 μ M concentration was indicated. ^b —, no inhibitory effect at 1 μ M.

Scheme 4, the substitution reaction proceeded and the corresponding 4-anilinoquinazolines **13** and **15–20** were obtained in high yields, except 4-(4'-hydroxymethylanilino)quinazoline **14** and 4-(3'-aminoanilino)quinazoline **21**. The compound **14** generated from **8** and 4-hydroxymethylaniline was gradually decomposed in air and the reaction of **8** with 1,4-diaminobenzene gave the corresponding 4-anilinoquinazoline **21** in only 17% yield. In the synthesis of 4-(4'-aminoanilino)quinazoline **23**, the first substitution reaction of **8** with Boc-protected 1,4-diaminobenzene was carried out and the resulting compound **22** was treated with trifluoromethanesulfonic acid (TFA) to give **23** in quantitative yield.

Table 2 shows the inhibition of a variety of functional groups substituted on the aniline moiety of 4-anilinoquinazolines, such as hydroxymethyl,²⁸ carboxylic acid, methyl ester, cyano, and amine groups, toward various tyrosine kinase activity. Interestingly, compound **19**, which has a cyano group substituted on a *meta* position of the aniline moiety, displayed high inhibition of EGFR tyrosine kinase (80%) similar to Tarceva (82%) at 1 μ M concentration, indicating that both cyano and acetylene groups can be similarly bound to the kinase pocket. In all cases except AAL993, significant inhibition of KDR tyrosine kinase was not observed at 1 μ M.



Since a boronic acid has been observed as an essential function for selective KDR kinase inhibition, we next examined whether

the boronic acids **9a–c** and **12a–c** are active species in the kinase assay. It has been reported that an aryl boronic acid is able to undergo oxidation with reactive oxygen species (ROS) in cells to be converted to phenols.²⁹ Furthermore, 4-(3'-hydroxyanilino)quinazoline **24**, which is considered as an oxidation product of the corresponding boronic acid **9a**, was reported as a selective KDR inhibitor (IC₅₀ = 0.05 μ M),³⁰ and 4-(4'-hydroxyanilino)quinazoline **25**, which may be generated from the corresponding boronic acid **12a** in a similar manner, was reported as a selective JAK3 inhibitor (IC₅₀ = 9.1 μ M).³¹ Therefore, we synthesized the *meta*-hydroxyl derivative **24** and the *para*-hydroxyl derivative **25** according to the literature procedures^{30,32} and examined the inhibition toward various tyrosine kinase activity. As shown in Table 2, the *meta*-hydroxyl derivative **24** exhibited inhibitory potency of broad-spectrum tyrosine kinases, whereas the *para*-hydroxyl derivative **25** did not display significant inhibitory activity toward these kinases at 1 μ M concentration. These results indicate that a boronic acid substituted on the aniline ring of the 4-anilinoquinazoline framework is essential for the selective inhibition of KDR tyrosine kinase.

Conclusions

We developed boronic acid-containing 4-anilinoquinazolines as selective inhibitors of EGFR and VEGFR2 tyrosine kinases. The substituted position of a boronic acid is essential for control of both kinase inhibitions. Since a boron atom is not observed in the living body, we believe that the current findings are promising for the utility of the boron atom as an alternative element in pharmaceutical drug design.

Notes and references

- P. Blume-Jensen and T. Hunter, *Nature*, 2001, **411**, 355–365.
- A. Levitzki, *Acc. Chem. Res.*, 2003, **36**, 462–469.
- R. A. LeMahieu, M. Carson, W. C. Nason, D. R. Parrish, A. F. Welton, H. W. Baruth and B. Yaremko, *J. Med. Chem.*, 1983, **26**, 420–425.
- D. W. Fry, A. J. Kraker, A. McMichael, L. A. Ambroso, J. M. Nelson, W. R. Leopold, R. W. Connors and A. J. Bridges, *Science*, 1994, **265**, 1093–1095.
- A. E. Wakeling, S. P. Guy, J. R. Woodburn, S. E. Ashton, B. J. Curry, A. J. Barker and K. H. Gibson, *Canc. Res.*, 2002, **62**, 5749–5754.
- M. Fukuoka, S. Yano, G. Giaccone, T. Tamura, K. Nakagawa, J.-Y. Douillard, Y. Nishiwaki, J. Vansteenkiste, S. Kudoh, D. Rischin, R. Eek, T. Horai, K. Noda, I. Takata, E. Smit, S. Averbuch, A. Macleod, A. Feyereislova, R.-P. Dong and J. Baselga, *J. Clin. Oncol.*, 2003, **21**, 2237–2246.
- J. D. Moyer, E. G. Barbacci, K. K. Iwata, L. Arnold, B. Boman, A. Cunningham, C. DiOrto, J. Doty, M. J. Morin, M. P. Moyer, M. Neveu, V. A. Pollack, L. R. Pustilnik, M. M. Reynolds, D. Sloan, A. Theleman and P. Miller, *Canc. Res.*, 1997, **57**, 4838–4848.
- F. A. Shepherd, J. Rodrigues Pereira, T. Ciuleanu, E. H. Tan, V. Hirsh, S. Thongprasert, D. Campos, S. Maoleekoonpiroj, M. Smylie, R. Martins, M. van Kooten, M. Dediu, B. Findlay, D. Tu, D. Johnston, A. Bezjak, G. Clark, P. Santabarbara, L. Seymour and the National Cancer Institute of Canada Clinical Trials Group, *N. Engl. J. Med.*, 2005, **353**, 123–132.
- L. Shewchuk, A. Hassell, B. Wisely, W. Rocque, W. Holmes, J. Veal and L. F. Kuyper, *J. Med. Chem.*, 2000, **43**, 133–138.
- J. Hong-Yun, W. Jiang-Xue, Z. Xiao-Feng, C. Jie-Min, Y. Shi-Ping, Y. Hai-Jiao, T. Li, Z. Yi-Xin and H. Wenlin, *Leuk. Res.*, 2009, **33**, 1512–1519.

- 11 K. Kubo, T. Shimizu, S.-i. Ohyama, H. Murooka, A. Iwai, K. Nakamura, K. Hasegawa, Y. Kobayashi, N. Takahashi, K. Takahashi, S. Kato, T. Izawa and T. Isoe, *J. Med. Chem.*, 2005, **48**, 1359–1366.
- 12 T. Furuta, T. Sakai, T. Senga, T. Osawa, K. Kubo, T. Shimizu, R. Suzuki, T. Yoshino, M. Endo and A. Miwa, *J. Med. Chem.*, 2006, **49**, 2186–2192.
- 13 N. Miyaura and A. Suzuki, *Chem. Rev.*, 1995, **95**, 2457–2483.
- 14 C. Kettner, L. Mersinger and R. Knabb, *J. Biol. Chem.*, 1990, **265**, 18289–18297.
- 15 S. Ness, R. Martin, A. M. Kindler, M. Paetzel, M. Gold, S. E. Jensen, J. B. Jones and N. C. J. Strynadka, *Biochemistry*, 2000, **39**, 5312–5321.
- 16 S. J. Coutts, T. A. Kelly, R. J. Snow, C. A. Kennedy, R. W. Barton, J. Adams, D. A. Krolikowski, D. M. Freeman, S. J. Campbell, J. F. Ksiazek and W. W. Bachovchin, *J. Med. Chem.*, 1996, **39**, 2087–2094.
- 17 K. A. Koehler and G. E. Lienhard, *Biochemistry*, 1971, **10**, 2477–2483.
- 18 W. Prusoff, T. S. Lin, A. Pivazyran, A. S. Sun and E. Birks, *Pharmacol. Ther.*, 1993, **60**, 315–329.
- 19 N. Suzuki, T. Suzuki, Y. Ota, T. Nakano, M. Kurihara, H. Okuda, T. Yamori, H. Tsumoto, H. Nakagawa and N. Miyata, *J. Med. Chem.*, 2009, **52**, 2909–2922.
- 20 D. S. Matteson, *Med. Res. Rev.*, 2008, **28**, 233–246.
- 21 A. F. Kisselev and A. L. Goldberg, *Chem. Biol.*, 2001, **8**, 739–758.
- 22 M. Groll, C. R. Berkers, H. L. Ploegh and H. Ovaa, *Structure*, 2006, **14**, 451–456.
- 23 H. S. Ban, T. Usui, W. Nabeyama, H. Morita, K. Fukuzawa and H. Nakamura, *Org. Biomol. Chem.*, 2009, **7**, 4415–4427.
- 24 M. D. Gaul, Y. Guo, K. Affleck, G. S. Cockerill, T. M. Gilmer, R. J. Griffin, S. Guntrip, B. R. Keith, W. B. Knight, R. J. Mullin, D. M. Murray, D. W. Rusnak, K. Smith, S. Tadepalli, E. R. Wood and K. Lackey, *Bioorg. Med. Chem. Lett.*, 2003, **13**, 637–640.
- 25 E. G. Barbacci, L. R. Pustilnik, A. M. Rossi, E. Emerson, P. E. Miller, B. P. Boscoe, E. D. Cox, K. K. Iwata, J. P. Jani, K. Provoncha, J. C. Kath, Z. Liu and J. D. Moyer, *Canc. Res.*, 2003, **63**, 4450–4459.
- 26 P. W. Manley, P. Furet, G. Bold, J. Brugger, J. Mestan, T. Meyer, C. R. Schnell, J. Wood, M. Haberey, A. Huth, M. Kruger, A. Menrad, E. Ottow, D. Seidelmann, G. Siemeister and K. H. Thierauch, *J. Med. Chem.*, 2002, **45**, 5687–5693.
- 27 J. S. Sebolt-Leopold and J. M. English, *Nature*, 2006, **441**, 457–462.
- 28 A. J. Barker, K. H. Gibson, W. Grundy, A. A. Godfrey, J. J. Barlow, M. P. Healy, J. R. Woodburn, S. E. Ashton, B. J. Curry, L. Scarlett, L. Henthorn and L. Richards, *Bioorg. Med. Chem. Lett.*, 2001, **11**, 1911–1914.
- 29 M. C. Y. Chang, A. Pralle, E. Y. Isacoff and C. J. Chang, *J. Am. Chem. Soc.*, 2004, **126**, 15392–15393.
- 30 L. F. Hennequin, A. P. Thomas, C. Johnstone, E. S. E. Stokes, P. A. Ple, J.-J. M. Lohmann, D. J. Ogilvie, M. Dukes, S. R. Wedge, J. O. Curwen, J. Kendrew and C. Lambert-van der Brempt, *J. Med. Chem.*, 1999, **42**, 5369–5389.
- 31 E. A. Sudbeck, X.-P. Liu, R. K. Narla, S. Mahajan, S. Ghosh, C. Mao and F. M. Uckun, *Clin. Canc. Res.*, 1999, **5**, 1569–1582.
- 32 G. W. Rewcastle, W. A. Denny, A. J. Bridges, H. Zhou, D. R. Cody, A. McMichael and D. W. Fry, *J. Med. Chem.*, 1995, **38**, 3482–3487.

Amphiphilic allylation of arylidene-1,3-oxazol-5(4*H*)-one using bis- π -allylpalladium complexes: an approach to synthesis of cyclohexyl and cyclohexenyl α -amino acids†Afaf R. Genady^a and Hiroyuki Nakamura^{*b}

Received 13th June 2011, Accepted 7th July 2011

DOI: 10.1039/c1ob05952a

An efficient method for synthesis of cyclohexyl and cyclohexenyl α -amino acids *via* palladium-catalyzed three-component assemblies followed by ring-closing metathesis (RCM) is described. The present catalytic reaction is successfully extended to substituted benzylidene azlactones **2a–j** RCH=(1,3-oxazole): R = alkyl or aryl. The amphiphilic bis-allylation of these substrates has been achieved by replacing toxic allylstannanes with allyltrifluoroborate and the reaction proceeded smoothly to afford the corresponding 1,7-diene derivatives **3a–j** in acceptable to good yields. RCM of the resulting octadienes using the first generation Grubbs catalyst gave easy access to stereodefined substituted cyclohexene derivatives **7–11** in high yields. Acid hydrolysis of the oxazolone ring of **7–10** gave protected amino acids **12–16**. Debenzoylation of **13** and **15** afforded 1-amino-6-aryl-cyclohex-3-enecarboxylic acids **17** and **18** in excellent yields, respectively. Moreover, catalytic reduction of **13** gave the corresponding cyclohexane derivative **19** which could be debenzoylated to give 1-amino-2-phenylcyclohexene-1-carboxylic acid (**20**). The structures of compounds **9**, **12** and **13** were confirmed by X-ray structural analysis. It is an excellent method for creating a wide range of cyclic α,α -disubstituted α -amino acids.

Introduction

Transition metal-catalyzed multicomponent assembling reactions provide an efficient route for the construction of complex organic molecules.¹ Catalytic transformations involving nucleophilic attack on (η^3 -allyl)palladium intermediates have been widely applied in a number of important chemical processes,^{2–7} including allylic substitution and the oxidation of alkenes and conjugated dienes. Palladium-catalyzed allylation with various nucleophiles (Tsuji–Trost-type reaction) is now a very important modern organic transformation for the construction of carbon–carbon or carbon–heteroatom bonds.⁸ Furthermore, it has been demonstrated that, under catalytic conditions, bis- π -allylpalladium complexes can undergo an initial electrophilic attack on one of the allyl moieties followed by a nucleophilic attack on the other.^{9–14} This bis- π -allylpalladium complex can act as an amphiphilic reagent reacting with activated olefins and arynes to form the corresponding

bis-allylation products. Subsequently, several modifications of this reaction with variation of allyl sources, activated alkenes and catalysts have been reported by different groups.^{15,16} This catalytic amphiphilic bis-allylation could also be applied to the synthesis of medium-sized carbocycles.¹⁷ Moreover, regioselective unsymmetrical tetra-allylation of C₆₀ was reported recently using the catalytic amphiphilic bis-allylation reaction.¹⁸

In the past decade, organotrifluoroborates have become important reagents in organoboron chemistry, in particular for transition-metal-catalyzed coupling reactions.^{16,19,20} These reagents are air- and thermostable species, which are usually easy to handle and purify. Moreover, allyltrifluoroborates have been shown to be effective allylating reagents for aldehydes.²² Recently, Batey and co-workers^{21,22} described the synthesis of a new class of allylboron compounds containing a trifluoroborate functionality. Due to the toxicity as well as the byproducts of organostannanes, we preferred the use of allyltrifluoroborate in catalytic bis- π -allylpalladium reactions. On the other hand, azlactones are important synthons for the synthesis of several biologically active compounds.²³ They are also particularly useful precursors for the synthesis of amino acids,²⁴ peptides,²⁵ heterocycles,²⁶ biosensors,²⁷ and antitumor²⁸ or anticancer²⁹ compounds.

The construction of suitably functionalized cyclohexene frameworks plays a central role in many natural product syntheses.³⁰ Although the Diels–Alder reaction is among the most powerful tools for generating such carbocycles,³¹ it is often difficult to form

^aDepartment of Chemistry, Faculty of Science, University of Tanta, 31527-Tanta, Egypt. E-mail: genadyafaf@yahoo.com

^bDepartment of Chemistry, Faculty of Science, Gakushuin University, 1-5-1 Mejiro, Toshima-ku, Tokyo 171-8588, Japan. E-mail: hiroyuki.nakamura@gakushuin.ac.jp; Fax: +81-3-5992-1029

† Electronic supplementary information (ESI) available: ¹H and ¹³C NMR spectra of compounds **3a–j** and **7–20**, and X-ray crystallographic files for compounds **9**, **12** and **13**. CCDC reference numbers 82954–82956. For ESI and crystallographic data in CIF or other electronic format see DOI: 10.1039/c1ob05952a

systems that are highly congested or possess substituent arrays that are incompatible with the reaction.³² A number of alternative methods for synthesizing cyclohexenes have arisen from catalytic approaches, such as the phosphine-catalyzed Rauhut–Currier reaction,³³ transition-metal-catalyzed ring-closing metathesis (RCM),³⁴ and cycloisomerization reactions.³⁵ In contradistinction to the widespread use of these intramolecular processes, intermolecular counterparts for catalytic cyclohexene synthesis are less well developed.^{36,37} With the development of air-stable, functionally compatible, and highly active ruthenium catalysts, such as the first-generation Grubbs catalyst³⁸ and second-generation Grubbs catalyst,³⁹ the ring-closing metathesis (RCM) reaction has become one of the most powerful methods to synthesize many kinds of cyclized products from acyclic diene or enyne precursors.⁴⁰ In this study, the first-generation Grubbs catalyst was used in the metathesis reaction of the resulting bis-allylated azlactones giving the corresponding cyclohexenes in excellent yields.

α,α -Disubstituted α -amino acids are nonproteinogenic modified amino acids, in which the hydrogen atom at the α -position of natural α -amino acids is replaced with an alkyl substituent.⁴¹ The α -alkyl substituents in α,α -disubstituted amino acids severely restrict the conformational freedom of peptides containing such residues, and these amino acids are used as a probe to investigate the biologically active conformation,⁴² to study the secondary structure of peptides,⁴³ and to search for the origin of chirality.⁴⁴ Furthermore, α,α -disubstituted α -amino acids are also found in many biologically active compounds, including antibiotics such as altamicidin.⁴⁵ Certain cyclic α,α -disubstituted amino acids, notably those with 3-, 5-, and 6-membered rings, tend to induce α -helical conformations when incorporated into peptides.⁴⁶ One of the challenges is to have procedures that provide flexible and simple methods for obtaining optically active α,α -disubstituted α -amino acids and that, furthermore, give diversity in structural and electronic properties.

Here we demonstrate a new protocol in amino acids synthesis; bis-allylated azlactones can act as excellent precursors for the synthesis of cyclic amino acids by bis-allylation of unsaturated azlactones. To the best of our knowledge, this is the first bis-allylation of azlactones. Catalytic cyclization of the resulting 1,7-diene afforded cyclohexene–azlactone adducts.

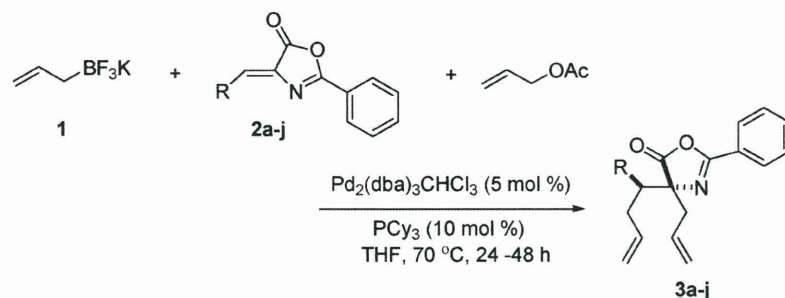
Results and discussion

Catalytic amphiphilic bis-allylation

The three-component assembling reactions such as bis-allylation gave the corresponding α,β -functionalized products in high yields. Although these reactions are limited to highly activated olefins,¹⁶ we succeeded in utilizing substituted azlactones **2a–j** as substrates. In the current study, we used an alternative catalytic system of bis- π -allylpalladium complexes generated from allyltrifluoroborate (**1**). Arylidene azlactones **2a–g** and **2i** were prepared according to the classic Erlenmeyer synthesis,⁴⁷ whereas **2h** and alkylidene azlactone **2j** were prepared under mild conditions using alumina as a catalyst.⁴⁸ In a preliminary study,⁴⁹ we reported suitable conditions for the amphiphilic bis-allylation of arylidene malononitrile with allyl acetate and allyltrifluoroborate to give substituted 1,7-diene derivatives. The results prompted us to extend this methodology into other olefins such as arylidene

azlactones in bis-allylation reactions as a masked amino acid fragment. Moreover, we examined the optimization of palladium catalysts and ligands for amphiphilic bis-allylation of activated alkenes by replacing allylstannanes with allyltrifluoroborate.⁴⁹ According to these results we found that the amphiphilic bis-allylation reaction with allyltrifluoroborate and allyl acetate proceeded smoothly using Pd₂(dba)₃CHCl₃/tricyclohexylphosphine (PCy₃) in THF. These reaction conditions could be applied to azlactones **2**. The reaction of benzylidene azlactone **2a** (1 equiv.), allyltrifluoroborate **1** (1.5 equiv.), and allyl acetate (1.5 equiv.) in THF proceeded in the presence of Pd₂(dba)₃CHCl₃ (5 mol%) and PCy₃ (10 mol%) in an argon atmosphere at 70 °C for 24 h to furnish 1,7-diene derivative **3a** in 45% yield. The low yield of **3a** could be explained by the formation of mono-allylated byproduct which was identified by ESI mass spectrometry. Increasing the reaction time had no effect on the bis-allylated yield. Moreover, allyl acetate gave the highest yield of three-component assembling product. Other substrates such as allyl chloride, which was considered the most appropriate for the amphiphilic bis-allylation with allyltributylstannane, were less effective for the reaction, affording **3a** in lower yield (26%). So, in another attempt to enhance the yield of the bis-allylated product, we performed the bis-allylation reaction using 3 equiv. of allyl acetate. It was found that the yield of **3a** increased to 49% (Table 1, entry 1). To study the scope of the reaction, attempting to enhance the activity of the double bond in azlactone, we used different aryl derivatives of azlactones. Several diversely substituted benzylidene azlactones underwent bis-allylations by this procedure to produce the corresponding 1,7-octadiene derivatives. The results are summarized in Table 1. This procedure is compatible with a wide range of substituents including electron donating and electron withdrawing groups substituted on the phenyl ring. Various substituted arylethylidene azlactones **2b–i** underwent bis-allylation with **1** and allyl acetate to give the corresponding three-component assembling products **3b–3i** in good yields (entries 2–9).

Arylethylidene azlactones with electron donating groups (entries 2–4) are more effective substrates for the assembling reaction than that bearing an electron withdrawing group on the phenyl ring (entry 5). The lower yield of **3d** compared to the yields of **3b** and **3c** was attributed to the insolubility of **2d** in THF and using DMF as the solvent (entry 4). The present protocol is successfully extended to azlactones with a heterocyclic substituent, such as furyl and pyridyl groups. Thus, treatment of furylidene azlactone (**2f**) and pyridylidene azlactone (**2h**) with **1** as well as allyl acetate in the presence of Pd₂(dba)₃CHCl₃/PCy₃ afforded the corresponding 1,7-diene derivatives **3f** and **3h** in 73% and 62% yields, respectively (entries 6 and 8). Under similar conditions, the reaction of piperonylidene azlactone (**2g**) with **1** and allyl acetate produced the corresponding assembling product **3g** in 75% yield (entry 7). The bis-allylation reaction also proceeded with *E/Z*-cinnamylidene azlactone **2i** to give (*E/Z*)-4-allyl-2-phenyl-4-(1-phenylhexa-1,5-dien-3-yl)oxazol-5(4*H*)-one (**3i**) in 32% yield (entry 9). It should be noted that the allylation reaction is completely regioselective, adding to the β and α carbons of **2i**. No other regioisomer was detected as evidenced by the ¹H NMR spectrum of the crude reaction mixture, indicating that the catalytic allylation is highly regioselective. The three-component assembling reaction of alkylidene azlactone **2j** gave **3j** in 68% yield (entry 10). The purification of the bis-allylation product was

Table 1 Palladium-catalyzed double allylation of olefins **2a–j** with allyltrifluoroborate **1** and allyl acetate

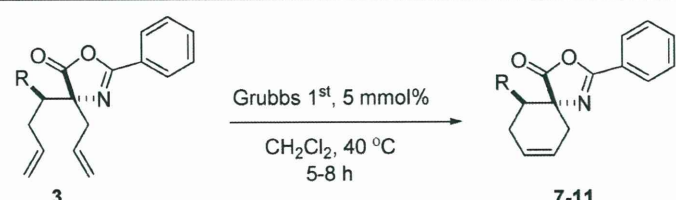
Entry	R	Product	Time (h)	Yield (%) ^a	d.r. ^b
1		3a	24	45	5:1
2		3b	24	58	4:1
3		3c	48	67	3:1
4		3d^c	24	47	3:1
5		3e	48	49	4:1
6		3f	24	73	5:1
7		3g	24	75	4:1
8		3h	24	62	3:1
9		3i	48	32	—
10		3j	24	68	4:1

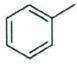
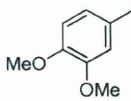

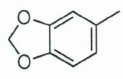
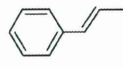
^a Combined isolated yields of two diastereomers based on **2**. ^b Diastereomer ratio determined by ¹H NMR. ^c DMF was used as the solvent.

performed by preparative thin layer chromatography (TLC) using hexane/ethyl acetate as the mobile phase. Diastereoselectivity (3–5:1) of the bis-allylation reactions was observed in all substituted azlactones **2a–j** except **2i** (Table 1). The major diastereomers were isolated by preparative TLC and identified.

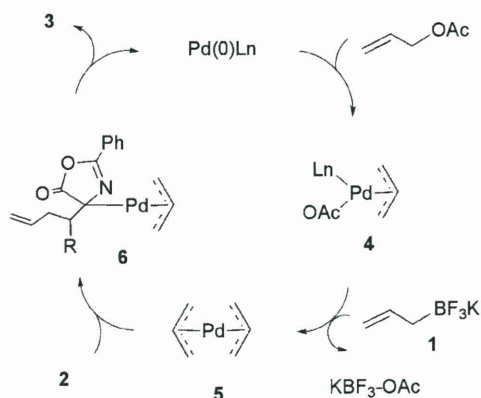
The proposed mechanism for the reaction course of this transformation is summarized in Scheme 1. On the basis of the known palladium chemistry and the mechanisms for the

catalytic reactions involving bis- π -allylpalladium complexes as key intermediates,^{9,17,50–52} a mechanism is proposed to account for the present catalytic amphiphilic bis-allylation reaction. The first step likely involves the oxidative addition of allyl acetate to Pd(0) to give π -allylpalladium acetate **4**. Transmetalation of allyltrifluoroborate **1** to π -allylpalladium acetate **4** gives bis- π -allylpalladium intermediate **5** and KBF₃OAc. Reaction of olefin **2** with **5** gives the complex **6**, which undergoes reductive elimination

Table 2 Metathesis reaction of **3**


Entry	3	Product	R	Yield (%) ^a
1	a 3	7		85
2	c 3	8		87
3	f 3	9		92
4	g 3	10		76
5	i 3	11		70

^a Isolated yields based on **3**.

**Scheme 1** Palladium-catalysis mechanism.

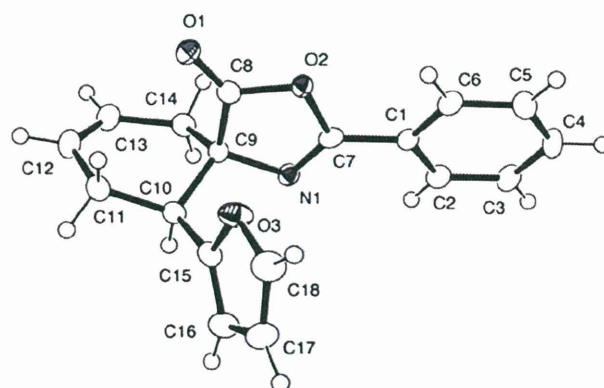
to afford the corresponding bis-allylated product **3** and regenerate the Pd(0) catalyst.

Metathesis of bis-allylated compounds

Catalytic olefin metathesis transformed some of these bis-allylated products (**3a**, **3c**, **3f**, **3g** and **3i**) to the corresponding cyclohexenes (**7–11**) in 70–92% yields (Table 2).

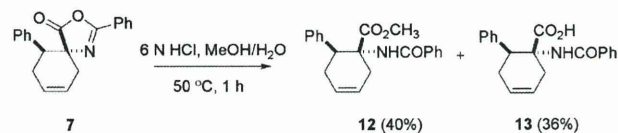
In our experiments the metathesis of bis-allylated products to cyclohexenes worked with excellent results when the reaction was carried out in dichloromethane at reflux for 5–8 h in the presence of 1st generation Grubbs' catalyst, allowing the formation of the corresponding cyclohexenes. The metathesis of **3i** is highly

chemoselective giving the cinnamyl-substituted product **11**, exclusively (entry 5). The ¹H NMR spectrum of compound **11** showed δ - and γ -CH protons resonate at 5.9 and 6.5 ppm, respectively. It was possible to obtain X-ray quality crystals from **9** by slow evaporation of a CH₂Cl₂/hexane solution at room temperature. The solid state structure of the cyclohexene **9**, determined by X-ray diffraction, is depicted in Fig. 1. The cyclohexene **9** consists of a cyclohexene ring having azlactone and furan moieties as substituents at positions 1 and 6. The C–C bond lengths of the cyclohexene ring span over a narrow range of 1.495(2)–1.555(2) Å compared with the C=C bond distance 1.322(2) Å.

**Fig. 1** ORTEP representation of **9**, showing 50% probability thermal ellipsoids.

Hydrolysis of oxazolone ring

One of the goals of our synthetic work was the successful preparation and characterization of a structurally diverse series of α,α -disubstituted α -amino acids derived from compounds 7–11. Incubation of azlactone 7 in a mixture of MeOH/H₂O (1 : 1) and HCl (6 N) at room temperature for 1 h resulted in cleavage of the oxazolone ring to give a mixture of 12 and 13 which could be isolated by preparative TLC to give 40% and 36% yields, respectively (Scheme 2).



Scheme 2 Cleavage of azlactone 7.

In the ¹H NMR spectra of 12 and 13, the new signals at 6.8 and 6.7 ppm indicated the presence of an NH group. ¹³C NMR spectra showed a low field shift of C=N of the former oxazolone ring in compounds 7–11, from *ca.* 160.2 ppm to *ca.* 166.8 ppm, whereas a high field shift of *ca.* 7 ppm for the carbonyl carbon of compounds 12 and 13 (172.8 ppm) compared with compound 7 (180.3 ppm) was observed. The expected deviations in these positions were attributed to oxazolone ring opening. Alternative conditions using a mixture of THF/aq. HCl (6 N) for direct conversion of 7 to the corresponding free carboxylic compound (13) were also possible. The compounds 12 and 13 crystallize in the monoclinic space groups *P*2₁/*c* and *C*2/*c*, respectively (Fig. 2, Table 3).

Similarly, compounds 8–10 were hydrolysed producing benzoylated amino acids 14–16 (Scheme 3). The structures of these compounds were also confirmed by both ¹H and ¹³C NMR spectroscopy, which showed the disappearance of the benzoyl CH and NH signals and appearance of high field NH₂ broad singlet at *ca.* 4.6 ppm. Amino acids 17 and 18 could be obtained from 13 and 15 in good yields by treatment with ammonia solution (Scheme 4).

Reduction of cyclohexene

Cyclohexene 13 was quantitatively hydrogenated in MeOH at room temperature, using 10% palladium/carbon as a catalyst to give cyclohexane 19, which is the direct precursor of the cyclohexane amino acid 20 (Scheme 4). The chemical shift of the CH=CH group of the former cyclohexene (compound 13) disappeared with appearance of new high field signals at 1.6 and 1.8 ppm of two methylene groups (compound 20) upon reduction. The ¹³C NMR spectrum showed new signals at approximately 25 ppm for the new methylene carbons of compound 20.

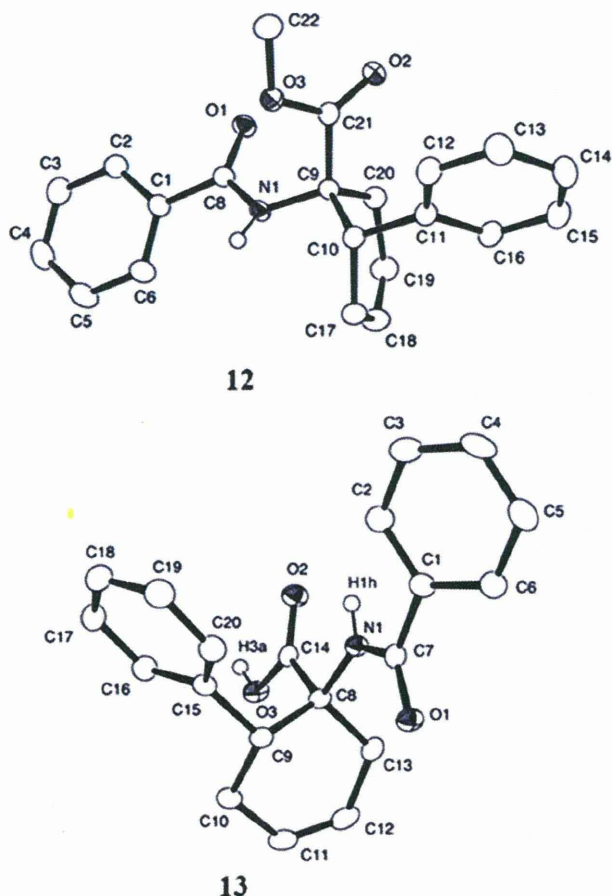
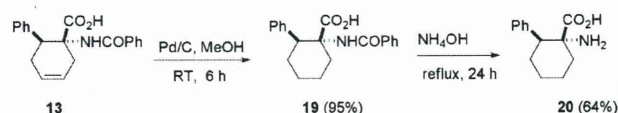
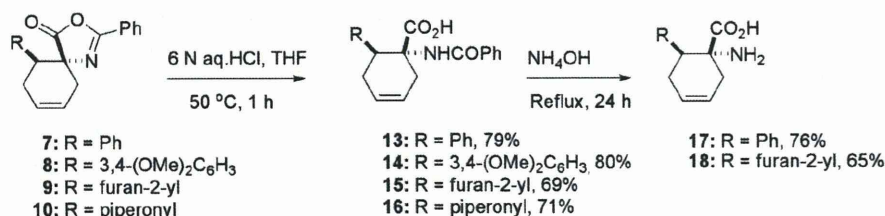


Fig. 2 X-Ray crystal structures of 12 and 13. Thermal probability ellipsoids are drawn at the 50% probability level (hydrogen atoms are omitted for clarity).



Scheme 4 Reduction of cyclohexene 13.

Azlactones and amino acids have characteristic stretching modes that are suitable for study by IR spectroscopy. The IR spectra of 3a–j contained weak and strong absorption bands located at *ca.* 1654, 1778, and 1816 cm⁻¹, which could be attributed to the vibrational modes of the C=C, C=N and C=O groups, respectively. These bands were not sensitive to the metathesis reactions in compounds 7–11. However, hydrolysis of azlactone followed by debenzoylation led to the complete disappearance of



Scheme 3 Conversion of azalactones to cyclic amino acids.

Table 3 Details of crystallographic data collection for **9**, **12** and **13**

	9	12	13
Formula	C ₁₈ H ₁₅ NO ₃	C ₂₂ H ₂₁ NO ₃	C ₂₀ H ₁₉ NO ₃
Fw	293.31	347.40	321.36
Crystal system	Orthorhombic	Monoclinic	Monoclinic
Space group	Fdd2	P2 ₁ /c	C2/c
a/Å	18.004(3)	10.6098(13)	29.149(6)
b/Å	39.249(6)	18.036(2)	7.5081(15)
c/Å	8.1408(11)	9.5122(12)	15.387(3)
α (°)	90	90	90
β (°)	90	98.7510(10)	107.300(2)
γ (°)	90	90	90
V/nm ³	5.7526(14)	1.7991(4)	3.2152(11)
Z	16	4	8
D _c /g cm ⁻³	1.355	1.283	1.328
F(000)	2464	736	1360
μ/mm ⁻¹	0.093	0.085	0.089
λ/Å	0.71073	0.71073	0.71073
Range (2θ) for data collection/°	2.08–27.57	2.25–27.46	2.77–27.52
GOF	1.675	1.027	1.03
T/K	123	123	123
R ₁ ^a (I > 2σ(I))	0.0391	0.0403	0.0448
wR ₂ ^b (I > 2σ(I))	0.0546	0.0985	0.0954
R ₁ ^a (all data)	0.0476	0.0495	0.0693
wR ₂ ^b (all data)	0.0557	0.1039	0.1059

^a R₁ = Σ||F_o| - |F_c||/Σ|F_o|. ^b wR₂ = [Σw(F_o² - F_c²)²/Σw(F_o²)²]^{1/2}.

the vibrational mode of C=N in the IR spectra of compounds **7–11**, which was replaced with a new strong absorption band (compounds **17**, **18** and **20**) at ca. 3500 cm⁻¹, which is characteristic of the NH₂ group, whereas ν(C=O) is shifted from ca. 1816 to 1725 cm⁻¹.

Conclusion

We have developed a procedure for the bis-allylation of activated azlactones via the three-component assembling reaction between arylidene azlactones, trifluoroborate and allyl acetate in the presence of palladium catalysts. In combination with our previously reported methodologies on the activated olefins, this methodology provides a novel process for the 1,2-bisfunctionalization of activated C=C bonds. This method allows an efficient synthesis of various 1,7-diene derivatives in good to excellent yields. The present catalytic reaction proceeds with various substituted azlactones. Metathesis cyclization of the resulting bis-allylated azlactones yielded the corresponding 3-oxa-1-aza-spiro[4.5]deca-1,7-dienes which could be either hydrolysed to the corresponding cyclohexenyl α-amino acids or reduced to the corresponding cyclohexyl α-amino acids.

Experimental section

Materials and methods

Most chemicals and solvents were of analytical grade and used without further purification. Aldehydes and Grubbs' catalyst were commercially available. Starting materials **1**, **2a–h** and **2i–j** were prepared as described in the literature.^{22,47,48} NMR spectra (¹H and ¹³C) were measured on 400 MHz spectrometer. Chemical shifts of ¹H NMR and ¹³C NMR were expressed in parts per million (ppm, δ units), and coupling constant (*J*) values were expressed in units

of hertz (Hz). IR (cm⁻¹) spectra were determined as KBr disc on an FTIR-8600PC spectrometer. Electron spray ionization (ESI) mass spectra were recorded on an LCMS-2010 eV spectrometer. Elemental analyses were performed by 2400 automatic elemental analyzer. All compounds gave elemental analysis within ±0.4% of the theoretical values. Analytical thin layer chromatography (TLC) was performed on glass plates of silica gel 60 GF₂₅₄. Visualization was accompanied by UV light (254 nm), I₂ or KMnO₄. Melting points (mp) were determined on ATM-01 melting point apparatus. Preparative TLC was carried out using 0.75 mm layers of silica gel 60 GF₂₅₄ made from water slurries on glass plates of dimensions 20 × 20 cm², followed by drying in air at 100 °C.

General procedure of amphiphilic bis-allylation of azlactone **2**

To a solution of azlactone **2** (0.65 mmol), allyltrifluoroborate (145 mg, 0.98 mmol), and Pd(dba)₃·CHCl₃ (35 mg, 0.033 mmol) in THF (10 ml) was added allyl acetate (2.1 ml, 1.96 mmol) and tricyclohexylphosphine (18 mg, 0.066 mmol) under nitrogen. The reaction mixture was heated with stirring at 70 °C for 24–48 h (TLC). The reaction was quenched with water, and the reaction mixture was extracted with ether, dried over anhydrous magnesium sulphate, and concentrated. Purification by preparative TLC with n-hexane/ethylacetate (9 : 1) as eluent gave the major diastereomer of bis-allylated product as a yellow oil.

Allyl-2-phenyl-4-(1-phenyl-but-3-enyl)-4H-oxazol-5-one (3a). Yield (97 mg, 45%); yellow oil; R_f 0.37 (n-hexane/AcOEt = 9 : 1); ¹H NMR (400 MHz, CDCl₃) δ 8.03 (d, 2H, *J* = 7.2 Hz), 7.57–7.28 (m, 8H), 5.45 (m, 2H), 5.02 (dd, 2H, *J* = 8 Hz, *J* = 3.5 Hz), 4.83 (dd, 2H, *J* = 8.0 Hz, *J* = 3.5 Hz), 3.18 (dd, 1H, *J* = 4.0 Hz, *J* = 4.0 Hz), 2.43 (m, 2H), 2.27 (m, 2H); ¹³C NMR (100 MHz, CDCl₃) δ 180.3, 160.2, 138.7, 135.2, 132.7, 130.5, 129.7, 128.8, 128.3, 128.0, 127.4, 125.8, 120.7, 117.1, 76.7, 52.1, 40.7, 36.2; IR (KBr disc) 3062, 2931, 1816, 1778, 1654, 972, 883, 702 cm⁻¹; MS, *m/z*

(ESI) 332.41 [100, M + 1]⁺; Anal. Calc. for C₂₂H₂₁NO₂: C, 79.73; H, 6.39; N, 4.23%. Found: C, 79.73; H, 6.32; N, 4.18%. ¹H NMR (400 MHz, CDCl₃) of the minor diastereomer: δ 7.98 (d, 2H, J = 7.00 Hz), 7.55–7.13 (m, 8H), 5.61 (m, 2H), 5.14 (dd, 2H, J = 8 Hz, J = 3.5 Hz), 4.95 (t, 2H, J = 7.5 Hz), 3.17 (dd, 1H, J = 4.0 Hz, J = 4.0 Hz), 2.67 (m, 2H), 2.51 (m, 2H).

4-Allyl-4-[1-(4-methoxy-phenyl)-but-3-enyl]-2-phenyl-4H-oxazol-5-one (3b). Yield (136 mg, 58%); yellow oil; R_f 0.53 (n-hexane/AcOEt = 9:1); ¹H NMR (400 MHz, CDCl₃) δ = 8.01 (d, 2H, J = 8.2 Hz), 7.55–7.43 (m, 3H), 7.38 (m, 2H), 7.23 (m, 2H), 5.49 (m, 2H), 5.16 (t, 2H, J = 10.5 Hz), 4.78 (t, 2H, J = 10.3 Hz), 3.75 (s, 3H), 3.23 (m, 1H), 2.43 (m, 2H), 2.23 (m, 2H); ¹³C NMR (100 MHz, CDCl₃) δ = 180.0, 162.3, 149.2, 147.7, 137.8, 136.6, 133.6, 129.4, 128.3, 128.3, 127.4, 125.6, 121.7, 115.0, 76.9, 55.8, 53.7, 39.4, 37.2; IR (KBr disc) 3065, 2935, 1808, 1774, 1655, 976, 885, 705 cm⁻¹; MS, m/z (ESI) 362.43 [100, M + 1]⁺; Anal. Calc. for C₂₃H₂₃NO₃: C, 76.43; H, 6.41; N, 3.88%. found: C, 76.32; H, 6.37; N, 3.79%. ¹H NMR (400 MHz, CDCl₃) of the minor diastereomer: δ = 7.90 (d, 2H, J = 8.0 Hz), 7.41–7.35 (m, 3H), 7.36 (m, 2H), 7.22 (m, 2H), 5.54 (m, 2H), 5.23 (t, 2H, J = 10.5 Hz), 4.71 (t, 2H, J = 10.3 Hz), 3.75 (s, 3H), 3.29 (m, 1H), 2.73 (m, 2H), 2.52 (m, 2H).

4-Allyl-4-[1-(3,4-dimethoxy-phenyl)-but-3-enyl]-2-phenyl-4H-oxazol-5-one (3c). Yield (170 mg, 67%); yellow oil; R_f 0.43 (n-hexane/AcOEt = 9:1); ¹H NMR (400 MHz, CDCl₃) δ = 8.03 (dd, 2H, J = 1.5 Hz, J = 1.5 Hz), 7.93 (d, 1H, J = 6.5 Hz), 7.57–7.49 (m, 3H), 6.84 (d, 1H, J = 8.0 Hz), 6.70 (m, 1H), 5.51 (m, 2H), 5.02 (t, 2H, J = 10.0 Hz), 4.86 (t, 2H, J = 10.0 Hz), 3.92 (s, 3H), 3.86 (s, 3H), 3.15 (m, 1H), 2.41 (m, 2H), 2.25 (m, 2H); ¹³C NMR (100 MHz, CDCl₃) δ = 179.3, 166.2, 149.2, 147.7, 137.6, 136.8, 133.1, 129.7, 128.8, 128.3, 127.4, 125.8, 121.6, 115.2, 77.0, 55.4, 55.2, 53.7, 39.5, 37.9; IR (KBr disc) 3058, 2936, 1812, 1772, 1655, 970, 882, 742 cm⁻¹; MS, m/z (ESI) 392.46 [100, M + 1]⁺; Anal. Calc. for C₂₄H₂₃NO₄: C, 73.64; H, 6.44; N, 3.58%. found: C, 73.59; H, 6.39; N, 3.47%. ¹H NMR (400 MHz, CDCl₃) of the minor diastereomer: δ = 7.93 (d, 2H, J = 4 Hz), 7.90 (d, 1H, J = 6.5 Hz), 7.54–7.45 (m, 3H), 6.83 (d, 1H, J = 8.0 Hz), 6.68 (m, 1H), 5.71 (m, 2H), 5.14 (t, 2H, J = 10.0 Hz), 4.79 (t, 2H, J = 10.0 Hz), 3.92 (s, 3H), 3.85 (s, 3H), 3.28 (m, 1H), 2.77 (m, 2H), 2.46 (m, 2H).

4-Allyl-4-[1-(4-dimethylamino-phenyl)-but-3-enyl]-2-phenyl-4H-oxazol-5-one (3d). Yield (114 mg, 47%); yellow oil; R_f 0.6 (n-hexane/AcOEt = 9:1); ¹H NMR (400 MHz, CDCl₃) δ = 8.07 (d, 2H, J = 3.5 Hz), 7.91 (d, 1H, J = 4.0 Hz), 7.73–7.40 (m, 5H), 5.47 (m, 2H), 4.99 (t, 2H, J = 7.5 Hz), 4.83 (t, 2H, J = 7.5 Hz), 3.17 (m, 1H), 2.99 (s, 3H), 2.83 (s, 3H), 2.42 (m, 2H), 2.23 (m, 2H); ¹³C NMR (100 MHz, CDCl₃) δ = 179.2, 168.3, 146.8, 137.6, 135.8, 131.5, 130.0, 129.6, 128.4, 127.4, 114.8, 115.7, 78.6, 40.5, 40.1, 35.8; IR (KBr disc) 3060, 2934, 1815, 1775, 1656, 987, 880, 725 cm⁻¹; MS, m/z (ESI) 375.48 [100, M + 1]⁺; Anal. Calc. for C₂₄H₂₆N₂O₂: C, 76.98; H, 7.00; N, 7.48%. found: C, 76.92; H, 6.97; N, 7.43%. ¹H NMR (400 MHz, CDCl₃) of the minor diastereomer: δ = 7.93 (d, 2H, J = 3.5 Hz), 7.90 (d, 1H, J = 4.0 Hz), 7.70–7.42 (m, 5H), 5.82 (m, 2H), 4.93 (t, 2H, J = 7.5 Hz), 4.80 (t, 2H, J = 7.5 Hz), 3.25 (m, 1H), 3.00 (s, 3H), 2.82 (s, 3H), 2.53 (m, 2H), 2.31 (m, 2H).

4-Allyl-4-[1-(4-nitro-phenyl)-but-3-enyl]-2-phenyl-4H-oxazol-5-one (3e). Yield (120 mg, 49%); yellow oil; R_f 0.42 (n-hexane/AcOEt = 9:1); ¹H NMR (400 MHz, CDCl₃) δ = 8.21

(d, 2H, J = 8.0 Hz), 8.04 (d, 2H, J = 8.0 Hz), 7.66–7.51 (m, 5H), 5.47 (m, 2H), 5.06 (dd, 2H, J = 9.0 Hz, J = 8.5 Hz), 4.86 (dd, 2H, J = 10.4 Hz, J = 9.6 Hz), 3.32 (dd, 1H, J = 6.0 Hz, J = 4.8 Hz), 2.45 (m, 2H), 2.20 (m, 2H); ¹³C NMR (100 MHz, CDCl₃) δ = 179.4, 160.7, 147.3, 146.5, 134.0, 133.0, 130.6, 129.7, 128.8, 128.0, 125.4, 123.5, 121.2, 118.0, 76.7, 51.5, 40.6, 36.0; IR (KBr disc) 3061, 2939, 1820, 1771, 1652, 976, 885, 741 cm⁻¹; MS, m/z (ESI) 454 [100, M + 2K]⁺; Anal. Calc. for C₂₂H₂₀N₂O₄: C, 70.20; H, 5.36; N, 7.44%. found: C, 70.17; H, 5.33; N, 7.40%. ¹H NMR (400 MHz, CDCl₃) of the minor diastereomer: δ = 8.13 (d, 2H, J = 8.0 Hz), 8.07 (d, 2H, J = 8.0 Hz), 7.66–7.51 (m, 5H), 5.61 (m, 2H), 5.14 (dd, 2H, J = 9.0 Hz, J = 8.5 Hz), 4.84 (dd, 2H, J = 10.4 Hz, J = 9.6 Hz), 3.74 (dd, 1H, J = 6.0 Hz, J = 4.8 Hz), 2.84 (m, 2H), 2.61 (m, 2H).

4-Allyl-4-(1-(furan-2-yl)but-3-enyl)-2-phenyloxazol-5(4H)-one (3f). Yield (152 mg, 73%); yellow oil; R_f 0.77 (n-hexane/AcOEt = 9:1); ¹H NMR (400 MHz, CDCl₃) δ = 8.00 (d, 2H, J_{CH} = 10.0 Hz), 7.58–7.47 (m, 3H), 7.35 (d, 1H, J = 8.0 Hz), 6.28 (d, 2H, J = 8.8 Hz) 5.57 (m, 2H), 5.12 (m, 2H), 4.85 (t, 2H, J = 10.0 Hz), 3.29 (m, 1H), 2.50 (m, 3H), 2.26 (m, 1H); ¹³C NMR (100 MHz, CDCl₃) δ = 178.4, 169.1, 157.7, 141.9, 137.6, 135.5, 131.4, 128.4, 115.7, 111.1, 105.7, 78.3, 43.5, 37.8, 29.6; IR (KBr) 3067, 2933, 1814, 1774, 1655, 973, 885, 719 cm⁻¹; MS, m/z (ESI) 321 [75, M]⁺; Anal. Calc. for C₂₀H₁₉NO₃: C, 74.75; H, 5.96; N, 4.36%. found: C, 74.62; H, 5.87; N, 4.27%. ¹H NMR (400 MHz, CDCl₃) of the minor diastereomer: δ = 7.96 (d, 2H, J_{CH} = 10.0 Hz), 7.56–7.48 (m, 3H), 7.31 (d, 1H, J = 8.0 Hz), 6.17 (d, 2H, J = 8.8 Hz) 5.73 (m, 2H), 5.07 (m, 2H), 4.81 (t, 2H, J = 10.0 Hz), 3.31 (m, 1H), 2.62 (m, 3H), 2.41 (m, 1H).

4-Allyl-4-(1-benzo[1,3]dioxol-5-yl-but-3-enyl)-2-phenyl-4H-oxazol-5-one (3g). Yield (182 mg, 75%); yellow oil; R_f 0.35 (n-hexane/AcOEt = 9:1); ¹H NMR (400 MHz, CDCl₃) δ = 8.04 (d, 2H, J = 8.0 Hz), 7.57–7.44 (m, 3H), 6.81–6.61 (m, 3H), 5.94 (s, 2H), 5.49 (m, 2H), 5.02 (m, 2H), 4.85 (m, 2H), 3.09 (m, 1H), 2.39 (m, 2H), 2.32 (m, 2H); ¹³C NMR (100 MHz, CDCl₃) δ = 177.7, 169.0, 148.5, 146.1, 136.8, 136.0, 132.7, 129.5, 128.7, 128.2, 121.6, 115.7, 113.6, 102.4, 78.6, 42.6, 42.3, 32.0; IR (KBr) 3066, 2932, 1815, 1775, 1656, 976, 885, 723 cm⁻¹; MS, m/z (ESI) 375.42 [100, M + 1]⁺; Anal. Calc. for C₂₃H₂₁NO₄: C, 73.58; H, 5.64; N, 3.73%. found: C, 73.53; H, 5.59; N, 3.71%. ¹H NMR (400 MHz, CDCl₃) of the minor diastereomer: δ = 7.91 (d, 2H, J = 8.0 Hz), 7.56–7.45 (m, 3H), 6.73–6.60 (m, 3H), 5.82 (s, 2H), 5.67 (m, 2H), 5.00 (m, 2H), 4.81 (m, 2H), 3.15 (m, 1H), 2.84 (m, 2H), 2.65 (m, 2H).

4-Allyl-2-phenyl-4-(1-(pyridin-4-yl)but-3-enyl)oxazol-5(4H)-one (3h). Yield (133 mg, 62%); yellow oil; R_f 0.45 (n-hexane/AcOEt = 9:1); ¹H NMR (400 MHz, CDCl₃) δ = 8.75 (d, 2H, J = 8.5 Hz), 8.25 (d, 2H, J = 8.5 Hz), 8.0 (d, 2H, J = 8.5 Hz), 7.72 (m, 1H), 7.51 (m, 2H), 5.65 (m, 2H), 4.95 (m, 2H), 4.81 (m, 2H), 3.19 (m, 1H), 2.49, 2.30 (m, 4H); ¹³C NMR (100 MHz, CDCl₃) δ = 180.2, 160.1, 154.0, 149.1, 139.0, 135.0, 129.6, 128.4, 126.3, 120.9, 117.1, 76.8, 52.1, 40.7, 36.2; IR (KBr disc) 3065, 2932, 1817, 1771, 1653, 975, 886, 722 cm⁻¹; MS, m/z (ESI) 333.40 [100, M + 1]⁺; Anal. Calc. for C₂₁H₂₀N₂O₂: C, 75.88; H, 6.06; N, 8.43%. found: C, 75.84; H, 6.03; N, 8.40%. ¹H NMR (400 MHz, CDCl₃) of the minor diastereomer: δ = 8.73 (d, 2H, J = 8.5 Hz), 8.25 (d, 2H, J = 8.5 Hz), 8.1 (d, 2H, J = 8.5 Hz), 7.68 (m, 1H), 7.53 (m, 2H), 5.74

(m, 2H), 5.06 (m, 2H), 4.92 (m, 2H), 3.27 (m, 1H), 2.64, 2.45 (m, 4H).

(*E/Z*)-4-allyl-2-phenyl-4-(1-phenylhexa-1,5-dien-3-yl)oxazol-5(4*H*)-one (3i). Yield (74 mg, 32%); yellow oil; R_f 0.5 (n-hexane/AcOEt = 9:1); $^1\text{H NMR}$ (400 MHz, CDCl_3) δ = 8.02 (d, 2H, J = 7.0 Hz), 7.61–7.21 (m, 8H), 6.55 (m, 1H), 6.21 (m, 1H), 5.63 (m, 2H), 5.12 (m, 4H), 3.31 (m, 1H), 2.75 (m, 2H), 2.45 (m, 2H); $^{13}\text{C NMR}$ (100 MHz, CDCl_3) δ = 179.8, 160.4, 136.7, 135.2, 134.4, 132.7, 130.5, 128.8, 128.5, 128.5, 128.0, 127.6, 127.3, 126.5, 126.4, 125.8, 120.7, 117.0, 76.5, 50.0, 40.7, 35.0; IR (KBr disc) 3065, 2937, 1815, 1778, 1659, 972, 886, 735 cm^{-1} ; MS, m/z (ESI) 356 [100, $\text{M} - 1$] $^-$; Anal. Calc. for $\text{C}_{24}\text{H}_{23}\text{NO}_2$: C, 80.64; H, 6.49; N, 3.92%. found: C, 80.59; H, 6.47; N, 3.87%. $^1\text{H NMR}$ (400 MHz, CDCl_3) of the minor diastereomer: δ = 8.00 (d, 2H, J = 7.0 Hz), 7.60–7.23 (m, 8H), 6.73 (m, 1H), 6.30 (m, 1H), 5.71 (m, 2H), 5.19 (m, 4H), 3.43 (m, 1H), 2.83 (m, 2H), 2.64 (m, 2H).

4-Allyl-4-(1-cyclohexylbut-3-enyl)-2-phenyloxazol-5(4*H*)-one (3j). Yield (138 mg, 63%); yellow oil; R_f 0.6 (n-hexane/AcOEt = 9:1); $^1\text{H NMR}$ (400 MHz, CDCl_3) δ = 8.04 (m, 2H), 7.64–7.41 (m, 3H), 5.53 (m, 2H), 5.02 (m, 2H), 4.86 (m, 2H), 3.26 (m, 1H), 2.97 (t, 1H, J = 10.0 Hz), 2.62, 2.38 (m, 4H), 2.23, 1.95 (m, 3H), 1.71–1.49 (m, 4H); $^{13}\text{C NMR}$ (100 MHz, CDCl_3) δ = 176.5, 167.2, 137.9, 136.1, 131.3, 128.4, 115.8, 76.5, 41.5, 33.2, 31.7, 29.4, 28.4, 28.3, 26.8; IR (KBr disc) 3062, 2939, 1822, 1779, 1656, 975, 887, 741 cm^{-1} ; MS, m/z (ESI) 337 [100, M] $^+$; Anal. Calc. for $\text{C}_{22}\text{H}_{27}\text{NO}_2$: C, 78.30; H, 8.06; N, 4.15%. found: C, 78.27; H, 8.03; N, 4.11%. $^1\text{H NMR}$ (400 MHz, CDCl_3) of the minor diastereomer: δ = 7.87 (m, 2H), 7.63–7.40 (m, 3H), 5.76 (m, 2H), 5.14 (m, 2H), 4.88 (m, 2H), 3.37 (m, 1H), 3.11 (t, 1H, J = 10.0 Hz), 2.83, 2.46 (m, 4H), 2.35, 2.06 (m, 3H), 1.82–1.68 (m, 4H).

General procedure for ring closing diene metathesis: synthesis of cyclohexene derivatives (7–11)

The typical procedure for the ring closing diene metathesis is as follows: precursor diene **3c**, **3f**, **3g**, or **3j** (1 mmol) was dissolved in freshly distilled and degassed dichloromethane (17 mL) under a nitrogen atmosphere. After stirring for 10 min at room temperature, ruthenium catalyst 1st generation (41.2 mg, 0.05 mmol) dissolved in dichloromethane (3 mL) was added by syringe. After 5–8 h of reflux at 40 °C, the reaction was complete as indicated by TLC. The solution was concentrated *via* rotavapor. TLC of the crude oil gave the corresponding cyclohexene derivatives as white solids.

2,10-Diphenyl-3-oxa-1-aza-spiro[4.5]deca-1,7-dien-4-one (7). Yield (257 mg, 85%); white solid; R_f 0.2 (n-hexane/AcOEt = 9:1); mp = 140–142 °C; $^1\text{H NMR}$ (300 MHz, CDCl_3) δ = 7.75 (d, 2H, J = 6.0 Hz), 7.46–7.10 (m, 8H), 6.04 (bs, 1H), 5.79 (bs, 1H), 3.45 (t, 1H, J = 6.6 Hz), 3.08 (t, 1H, J = 15.0 Hz), 2.90 (d, 1H, J = 18.0 Hz), 2.45 (t, 2H, J = 18.0 Hz); $^{13}\text{C NMR}$ (100 MHz, CDCl_3) δ = 177.0, 161.0, 138.4, 136.4, 131.6, 128.6, 126.7, 68.5, 39.0, 34.2, 27.6; IR (KBr disc) 3065, 2935, 1825, 1775, 1658, 1045, 887, 742 cm^{-1} ; MS, m/z (ESI) 304 [100, $\text{M} + 1$] $^+$. Anal. Calc. for $\text{C}_{20}\text{H}_{17}\text{NO}_2$: C, 79.19; H, 5.65; N, 4.62%. found: C, 79.11; H, 5.58; N, 4.57%.

10-(3,4-Dimethoxy-phenyl)-2-phenyl-3-oxa-1-aza-spiro[4.5]deca-1,7-dien-4-one (8). Yield (315 mg, 87%); white solid; R_f 0.15

(n-hexane/AcOEt = 9:1); mp = 134–136 °C; $^1\text{H NMR}$ (400 MHz, CDCl_3) δ = 7.76 (t, 2H, J = 6.5 Hz), 7.47–7.34 (m, 4H), 6.79–6.69 (m, 2H), 6.05 (m, 1H), 5.68 (m, 1H), 3.78 (s, 3H), 3.74 (s, 3H), 3.40 (dd, 1H, J = 6.0, 6.5 Hz), 3.05 (t, 1H, J = 12.0 Hz), 2.85 (m, 1H), 2.43 (t, 2H, J = 12.0 Hz); $^{13}\text{C NMR}$ (100 MHz, CDCl_3) δ = 177.0, 163.2, 147.6, 146.0, 136.4, 132.0, 128.6, 126.3, 115.8, 68.2, 54.5, 40.0, 33.8, 27.4; IR (KBr disc) 3059, 2928, 1810, 1775, 1652, 1025, 887, 738 cm^{-1} ; MS, m/z (ESI) 364 [100, $\text{M} + 1$] $^+$; Anal. Calc. for $\text{C}_{22}\text{H}_{21}\text{NO}_4$: C, 72.71; H, 5.82; N, 3.85%. found: C, 72.63; H, 5.77; N, 3.81%.

10-Furan-2-yl-2-phenyl-3-oxa-1-aza-spiro[4.5]deca-1,7-dien-4-one (9). Yield (269 mg, 92%); white solid; R_f 0.25 (n-hexane/AcOEt = 9:1); mp = 131–133 °C; $^1\text{H NMR}$ (400 MHz, CDCl_3) δ = 7.86 (d, 2H, J = 8 Hz), 7.52–7.49 (m, 1H), 7.43–7.40 (m, 2H), 7.18 (s, 1H), 6.15 (dd, 2H, J = 8.0, 6.5 Hz), 5.96 (m, 1H), 5.73 (m, 1H), 3.55 (t, 1H, J = 10.0 Hz), 2.95 (t, 1H, J = 12.0 Hz), 2.78 (d, 1H, J = 12.5 Hz), 2.42 (m, 2H); $^{13}\text{C NMR}$ (100 MHz, CDCl_3) δ = 177.2, 161.5, 153.3, 141.7, 132.6, 128.6, 127.8, 127.0, 125.7, 121.2, 110.0, 106.0, 69.4, 40.0, 33.7, 27.3; IR (KBr disc) 3057, 2932, 1821, 1775, 1656, 975, 889, 729 cm^{-1} ; MS, m/z (ESI) 295 [100, $\text{M} + 2\text{H}$] $^+$; Anal. Calc. for $\text{C}_{18}\text{H}_{15}\text{NO}_3$: C, 73.71; H, 5.15; N, 4.78%. found: C, 73.68; H, 5.11; N, 4.75%.

10-Benzo[1,3]dioxol-5-yl-2-phenyl-3-oxa-1-aza-spiro[4.5]deca-1,7-dien-4-one (10). Yield (263 mg, 76%); white solid; R_f 0.3 (n-hexane/AcOEt = 9:1); mp = 165–167 °C; $^1\text{H NMR}$ (400 MHz, CDCl_3) δ = 7.97 (m, 2H), 7.46–7.34 (m, 4H), 6.72–6.53 (m, 3H), 6.02 (m, 1H), 5.87 (m, 2H), 5.72 (m, 1H), 3.37 (q, 1H, J = 8.0 Hz), 2.96 (t, 1H, J = 11.5 Hz), 2.79 (d, 1H, J = 11.5 Hz), 2.39 (m, 2H); $^{13}\text{C NMR}$ (100 MHz, CDCl_3) δ = 178.0, 162.8, 148.0, 146.7, 136.6, 135.7, 132.6, 129.6, 128.9, 121.3, 115.7, 113.4, 101.8, 68.5, 40.6, 36.0, 28.0; IR (KBr disc) 3065, 2935, 1813, 1772, 1654, 972, 885, 725 cm^{-1} ; MS, m/z (ESI) 347 [100, M] $^+$; Anal. Calc. for $\text{C}_{20}\text{H}_{17}\text{NO}_4$: C, 72.61; H, 4.93; N, 4.03%. found: C, 72.58; H, 4.88; N, 3.99%.

2-Phenyl-10-styryl-3-oxa-1-aza-spiro[4.5]deca-1,7-dien-4-one (11). Yield (230 mg, 70%); white solid; R_f 0.28 (n-hexane/AcOEt = 9:1); mp = 172–174 °C; $^1\text{H NMR}$ (400 MHz, CDCl_3) δ = 7.94 (m, 2H), 7.54–7.41 (m, 3H), 7.22–7.15 (m, 5H), 6.54 (m, 1H), 5.94 (m, 2H), 5.73 (m, 1H), 2.96 (m, 1H), 2.64 (m, 2H), 2.44 (m, 2H); $^{13}\text{C NMR}$ (100 MHz, CDCl_3) δ = 177.8, 160.3, 136.8, 134.1, 133.7, 129.0, 128.7, 128.4, 128.1, 126.5, 126.4, 126.3, 125.8, 122.0, 121.3, 69.7, 43.5, 42.9, 34.5, 32.8, 28.5, 27.7; IR (KBr disc) 3068, 2932, 1815, 1775, 1656, 977, 889, 741 cm^{-1} ; MS, m/z (ESI) 352 [100, $\text{M} + \text{Na}$] $^+$; Anal. Calc. for $\text{C}_{22}\text{H}_{19}\text{NO}_2$: C, 80.22; H, 5.81; N, 4.25%. found: C, 80.19; H, 5.79; N, 4.21%.

General procedure of hydrolysis of azlactones

Method A. 6 N aq. HCl (10 mL) was added to a solution of azlactone **7** (303 mg, 1 mmol) in 10 mL methanol at room temperature in a 50 mL round flask. The reaction mixture was heated at 50 °C for 1 h and the formation of the products was monitored by TLC. The solvents were evaporated under vacuum to yield a white solid of the crude product which was purified by preparative TLC using CH_2Cl_2 /methanol (90:5) as eluent to yield colorless crystalline solids.

Method B. A solution of aq. HCl (6 M, 10 mL) was added to a solution of azlactone **7**, **8**, **10** or **11** (1 mmol) in 5 mL THF at room temperature in a 25 mL round flask. The reaction mixture was heated at 70 °C for 1 h and the formation of the products was monitored by TLC. The solvents were evaporated under vacuum to yield a white solid of the crude product which was purified by preparative TLC using CH₂Cl₂/methanol (90 : 5) as eluent to yield colorless solids.

Methyl(1-benzoylamino-6-phenyl-cyclohex-3-enecarboxylate) (12). Yield (134 mg, 40%); white solid; *R_f* 0.57 (CH₂Cl₂/MeOH = 90 : 5); mp = 153–155 °C; ¹H NMR (400 MHz, CDCl₃) δ = 7.67 (d, 2H, *J* = 6 Hz), 7.47–7.16 (m, 8H), 6.79 (s, 1H), 5.9 (m, 1H), 5.82 (m, 1H), 3.72 (m, 1H), 3.69 (s, 3H), 3.15 (d, 1H, *J* = 8.5 Hz), 2.74 (d, 1H, *J* = 8.5 Hz), 2.61 (m, 2H); ¹³C NMR (100 MHz, CDCl₃) δ = 172.7, 166.8, 140.2, 134.7, 131.5, 128.5, 128.4, 128.1, 127.5, 126.9, 125.3, 125.0, 61.7, 43.8, 29.9, 29.3; IR (KBr disc) 3389, 3059, 2929, 1725, 1685, 1645, 979, 882, 742 cm⁻¹; MS, *m/z* (ESI) 358 [100, M + Na]⁺; Anal. Calc. for C₂₁H₂₁NO₃: C, 75.2; H, 6.31; N, 4.18%. found: C, 74.93; H, 6.15; N, 4.07%.

1 - Benzoylamino - 6 - phenyl - cyclohex - 3 - enecarboxylic acid (13). Yield (253 mg, 79%); white solid; *R_f* 0.15 (CH₂Cl₂/MeOH = 90 : 5); mp = 219–221 °C; ¹H NMR (400 MHz, CDCl₃) δ = 7.69 (d, 2H, *J* = 6.3 Hz), 7.54 (m, 2H), 7.43 (m, 2H), 7.28 (m, 6H), 6.73 (s, 1H), 6.01 (m, 1H), 5.85 (m, 1H), 4.06 (m, 1H), 2.77 (t, 2H, *J* = 8.0 Hz), 2.60 (t, 2H, *J* = 8.0 Hz); ¹³C NMR (100 MHz, CDCl₃) δ = 175.5, 165.8, 141.1, 135.6, 131.9, 128.5, 128.4, 128.2, 127.5, 126.9, 125.3, 124.9, 61.7, 43.9, 30.2, 30.1; IR (KBr disc) 3391, 3057, 2931, 1727, 1681, 1642, 974, 887, 740 cm⁻¹; MS, *m/z* (ESI) 344 [100, M + Na]⁺; Anal. Calc. for C₂₀H₁₉NO₃: C, 74.75; H, 5.96; N, 4.36%. found: C, 74.71; H, 5.93; N, 4.34%.

1-Benzoylamino-6-(3,4-dimethoxy-phenyl)-cyclohex-3-enecarboxylic acid (14). Yield (305 mg, 80%); white solid; *R_f* 0.42 (CH₂Cl₂/MeOH = 90 : 5); mp = 195–197 °C; ¹H NMR (400 MHz, CDCl₃) δ = 7.68–7.49 (m, 4H), 6.86–6.72 (m, 4H), 6.25 (s, 1H), 5.90 (m, 1H), 5.75 (m, 1H), 3.83 (m, 1H), 3.76 (s, 3H), 3.74 (s, 3H), 3.21 (d, 1H, *J* = 12.0 Hz), 2.75–2.62 (m, 3H); ¹³C NMR (100 MHz, CDCl₃) δ = 172.8, 167.5, 147.6, 146.3, 135.2, 131.5, 127.2, 125.0, 116.6, 62.2, 54.3, 42.0, 39.5, 28.4; IR (KBr disc) 3395, 3062, 2932, 1727, 1682, 1647, 975, 886, 741 cm⁻¹; MS, *m/z* (ESI) 382 [100, M + 1]⁺; Anal. Calc. for C₂₂H₂₃NO₃: C, 69.28; H, 6.08; N, 3.67%. found: C, 69.24; H, 6.03; N, 3.65%.

1 - Benzoylamino - 6 - furan - 2 - yl - cyclohex - 3 - enecarboxylic acid (15). Yield (214 mg, 69%); white solid; *R_f* 0.23 (CH₂Cl₂/MeOH = 90 : 5); mp = 201–203 °C; ¹H NMR (400 MHz, CDCl₃) δ = 7.73 (d, 2H, *J* = 6.8 Hz), 7.53–7.31 (m, 4H), 7.26 (s, 1H), 6.29 (d, 2H, *J* = 7.2 Hz), 6.20 (s, 1H), 5.85 (m, 2H), 4.14 (bs, 1H), 2.96 (bs, 1H), 2.74–2.52 (m, 3H); ¹³C NMR (100 MHz, CDCl₃) δ = 175.5, 162.1, 139.5, 136.4, 130.3, 128.7, 126.0, 63.9, 38.8, 33.8, 25.2; IR (KBr disc) 3397, 3056, 2935, 1725, 1686, 1645, 975, 886, 745 cm⁻¹; MS, *m/z* (ESI) 334 [60, M + Na]⁺; Anal. Calc. for C₁₈H₁₇NO₄: C, 69.44; H, 5.50; N, 4.50%. found: C, 69.40; H, 5.48; N, 4.47%.

6-Benzo[1,3]dioxol-5-yl-1-benzoylamino-cyclohex-3-enecarboxylic acid (16). Yield (259 mg, 71%); white solid; *R_f* 0.26 (CH₂Cl₂/MeOH = 90 : 5); mp = 187–189 °C; ¹H NMR (400 MHz, CDCl₃) δ = 7.63–7.25 (m, 5H), 6.78–6.59 (m, 4H), 5.79 (m, 4H),

3.91 (bs, 1H), 3.00 (bs, 1H), 2.58 (m, 3H); ¹³C NMR (100 MHz, CDCl₃) δ = 174.1, 163.5 (C=N), 151.5, 148.1, 140.2, 135.7, 131.7, 128.2, 127.0, 125.5, 122.3, 115.6, 107.8, 100.6, 64.4, 44.6, 34.2, 30.3, 21.1; IR (KBr disc) 3400, 3065, 2935, 1724, 1685, 1643, 977, 885, 742 cm⁻¹; MS, *m/z* (ESI) 366 [100, M + 1]⁺; Anal. Calc. for C₂₁H₁₉NO₅: C, 69.03; H, 5.24; N, 3.83%. found: C, 69.00; H, 5.21; N, 3.79%.

General procedures for debenzoylation of compounds **13** and **16**

Ammonium hydroxide solution (3 mL) was added to a solution of **13** or **16** (1 mmol) in methanol (15 mL) at room temperature. The mixture was refluxed for 24 h. When the reaction mixture had reached room temperature, the solvents were evaporated under vacuum and the crude substance was purified by TLC using CH₂Cl₂/methanol (80 : 20) as the mobile phase to give cream colored solids.

1-Amino-6-phenyl-cyclohex-3-enecarboxylic acid (17). Yield (165 mg, 76%); white solid; *R_f* 0.24 (CH₂Cl₂/Methanol = 9 : 1); mp = 219–221 °C; ¹H NMR (400 MHz, CDCl₃) δ = 7.73, 7.63, 7.40 (m, 5H), 6.08 (m, 1H), 5.81 (m, 1H), 4.51 (bs, 2H), 4.05 (m, 1H), 2.85 (m, 2H), 2.60 (m, 2H); ¹³C NMR (100 MHz, CDCl₃) δ = 178.5, 138.2, 129.2, 129.0, 127.8, 126.8, 126.0, 71.1, 46.8, 31.1, 27.5; IR (KBr disc) 3512, 3052, 2937, 1705, 1645, 979, 882, 743 cm⁻¹; MS, *m/z* (ESI) 240 [100, M + Na]⁺; Anal. Calc. for C₁₃H₁₅NO₂: C, 71.87; H, 6.96; N, 6.45%. found: C, 71.84; H, 6.93; N, 6.41%.

1-Amino-6-furan-2-yl-cyclohex-3-enecarboxylic acid (18). Yield (134 mg, 65%); white solid; *R_f* 0.21 (CH₂Cl₂/Methanol = 9 : 1); mp = 179–181 °C; ¹H NMR (400 MHz, CDCl₃) δ = 7.39 (d, 1H, *J* = 8.0 Hz), 6.08 (d, 2H, *J* = 8.2 Hz), 5.95 (m, 1H), 5.73 (m, 1H), 4.68 (bs, 2H), 3.38 (d, 1H, *J* = 9.5 Hz), 2.98–2.77 (m, 2H), 2.41–2.35 (m, 2H); ¹³C NMR (100 MHz, CDCl₃) δ = 175.6, 139.6, 136.5, 63.9, 38.8, 33.8, 25.2; IR (KBr disc) 3507, 3058, 2931, 1697, 1641, 976, 884, 742 cm⁻¹; MS, *m/z* (ESI) 230 [97, M + Na]⁺; Anal. Calc. for C₁₁H₁₃NO₃: C, 63.76; H, 6.32; N, 6.76%. found: C, 63.61; H, 6.27; N, 6.71%.

Synthesis of 1-benzamido-2-phenylcyclohexanecarboxylic acid (19)

To a mixture of **13** (0.16 g, 0.5 mmol) and Pd/C (0.058 g) in dry MeOH (10 mL) solution was added one drop of AcOH under hydrogen atmosphere, and the reaction mixture was stirred at room temperature for 6 h. The palladium catalyst was removed by filtration through Celite, and the solvent was evaporated. The white solid was washed with CH₂Cl₂ to afford **19**. Yield (153 mg, 95%); mp = 208–210 °C; ¹H NMR (400 MHz, CDCl₃) δ = 7.69–7.40 (m, 5H), 7.16 (m, 5H), 3.85 (d, 1H, *J* = 9.2 Hz), 2.75 (q, 1H, *J* = 8.0 Hz), 2.46 (q, 1H, *J* = 8.0 Hz), 2.10 (t, 2H, *J* = 14.0 Hz), 1.93 (d, 1H, *J* = 12.0 Hz), 1.78 (t, 2H, *J* = 12.0 Hz), 1.57 (m, 1H); ¹³C NMR (100 MHz, CDCl₃) δ = 174.5, 166.1, 145.1, 134.0, 133.2, 127.0, 126.9, 126.4, 125.7, 62.0, 45.5, 29.3, 24.9, 20.5; IR (KBr disc) 3393, 3059, 2932, 1725, 1682, 975, 885, 741 cm⁻¹; MS, *m/z* (ESI) 346 [100, M + Na]⁺; Anal. Calc. for C₂₀H₂₁NO₃: C, 74.28; H, 6.55; N, 4.33%. found: C, 74.24; H, 6.51; N, 4.30%.

1-Amino-2-phenyl-cyclohexanecarboxylic acid (20). This compound was prepared from **19** (323 mg, 1 mmol) and ammonium hydroxide solution (3 mL), using the debenzoylation procedure described for **13** to give **20** as a white solid.

Yield (140 mg, 64%); white solid; R_f 0.17 (CH₂Cl₂/Methanol = 9:1); mp = 165–167 °C; ¹H NMR (400 MHz, CDCl₃) δ = 8.00 (d, 2H, J = 6.0 Hz), 7.62 (m, 3H), 4.21 (m, 1H), 3.85 (bs, 2H), 2.83 (t, 1H, J = 12.0 Hz), 2.43 (m, 1H), 2.20 (t, 2H, J = 12.0 Hz), 1.91–1.76 (m, 4H); ¹³C NMR (100 MHz, CDCl₃) δ = 176.0, 147.1, 128.0, 126.5, 126.4, 63.5, 43.0, 29.0, 25.1, 19.3; IR (KBr disc) 3503, 3062, 2933, 1706, 973, 885, 742 cm⁻¹; MS, m/z (ESI) 242 [93, M + Na]⁺; Anal. Calc. for C₁₃H₁₇NO₂: C, 71.21; H, 7.81; N, 6.39%. found: C, 71.20; H, 7.81; N, 6.37%.

Crystal structure determination of 9, 12 and 13

Colorless single crystals of **9** suitable for XRD analyses were obtained from slow evaporation of a CH₂Cl₂/hexanes solution at room temperature. However, colorless crystals of **12** and **13** were obtained by slow evaporation of methanol solutions at room temperature. Each crystal was mounted on a glass fiber, and the diffraction data of all the complexes were collected on an AXS APEX II CCD detector using graphite monochromated Mo-K α radiation at 123 K. The crystal data and experimental details are listed in Table 3. All the structures were solved by the combination of direct methods and Fourier techniques, and all the non-hydrogen atoms were anisotropically refined by full-matrix least-squares calculations. The atomic scattering factors and anomalous dispersion terms were obtained from the International Tables for X-ray Crystallography IV.⁵³ Since the reflection data for the abovementioned crystals were insufficient for refining all the parameters of the hydrogen atoms, they were obtained from difference Fourier maps.

Acknowledgements

We thank Dr Hidekazu Arii (Gakushuin University) for the crystal structure artwork.

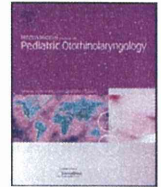
References

- (a) J. Tsuji, *Transition Metal Reagents and Catalysts: Innovations in Organic Synthesis*, Wiley, New York, 2002; (b) L. S. Hegedus, *Transition Metals in the Synthesis of Complex Organic Molecules*, 2nd ed. University Science Books, Sausalito, CA, 1999; (c) J. Montgomery and Acc. Chem. Res., 2000, **33**, 467; (d) S. I. Ikeda, *Acc. Chem. Res.*, 2000, **33**, 511.
- (a) Z. Wang, X. Lu, A. Lei and Z. Zhang, *J. Org. Chem.*, 1998, **63**, 3806; (b) N. Chatani, N. Amishiro and S. Murai, *J. Am. Chem. Soc.*, 1991, **113**, 7778; (c) S. A. Codleski, In *Comprehensive Organic Synthesis*, M. F. Semmelhack, Ed.; Pergamon Press, Oxford, 1991, **4**, 585.
- J. P. Collman, L. S. Hegedus, J. R. Norton and R. G. Finke, In *Principles and Applications of Organotransition Metal Chemistry*, University Science Books, Mill Valley, 1987, 417.
- S. A. Godleski, *Comprehensive Organic Synthesis* B. M. Trost and I. Fleming, Ed.; Pergamon Press, New York, 1991, **4**, Chapter 3.3.
- P. J. Harrington, *Comprehensive Organometallic Chemistry II*, E. W. Abel, F. Gordon, A. Stone, G. Wilkinson and R. J. Puddephatt, ed.; Elsevier, New York, 1995, **12**, 797.
- J.-E. Bäckvall, *Metal-catalyzed Cross Coupling Reactions*, VCH, Weinheim, 1998, 339.
- B. M. Trost, *Acc. Chem. Res.*, 1980, **13**, 385.
- J. Tsuji, *Palladium Reagents and Catalysis: Innovations in Organic Synthesis*, Wiley, Chichester, 1995; Chapters 3 and 4.
- H. Nakamura, J.-G. Shim and Y. Yamamoto, *J. Am. Chem. Soc.*, 1997, **119**, 8113.
- H. Nakamura, K. Nakamura and Y. Yamamoto, *J. Am. Chem. Soc.*, 1998, **120**, 4242.
- K. Nakamura, H. Nakamura and Y. Yamamoto, *J. Org. Chem.*, 1999, **64**, 2614.
- K. Ohno and J. Tsuji, *J. Chem. Soc. D*, 1971, 247.
- J. Kiji, K. Yamamoto, H. Tomita and J. Furukawa, *J. Chem. Soc., Chem. Commun.*, 1974, 506.
- K. Ohno, T. Mitsuyasu and J. Tsuji, *Tetrahedron*, 1972, **28**, 3705.
- Y. Tamaru, *Eur. J. Org. Chem.*, 2005, **13**, 2647.
- M. Jeganmohan, M. Shanmugasundaram and C.-H. Cheng, *J. Org. Chem.*, 2004, **69**, 4053.
- H. Nakamura, K. Aoyagi, J.-G. Shim and Y. Yamamoto, *J. Am. Chem. Soc.*, 2001, **123**, 372.
- M. Nambo, A. Wakamiya, S. Yamaguchi, K. Itami and K. Szabó, *J. Am. Chem. Soc.*, 2009, **131**, 15112.
- G. A. Molander and R. Figueroa, *Aldrichim. Acta*, 2005, **38**, 49.
- S. Darses and J. P. Genet, *Chem. Rev.*, 2008, **108**, 288.
- R. A. Batey, A. N. Thadani, D. V. Smil and A. J. Lough, *Synthesis*, 2000, 990.
- R. A. Batey, A. N. Thadani and D. V. Smil, *Tetrahedron Lett.*, 1999, **40**, 4289.
- K. Takenaka and T. Tsuji, *J. Heterocycl. Chem.*, 1996, **33**, 1367.
- J. T. Konkel, J. Fan, B. Jayachandran and K. L. Kirk, *J. Fluorine Chem.*, 2002, **115**, 27.
- F. Caveller and J. Verducci, *Tetrahedron Lett.*, 1995, **36**, 4425.
- A. Avenoza, J. H. Pusto, C. Cativiela and J. M. Peregrina, *Tetrahedron Lett.*, 2002, **36**, 4167.
- S. Kozima, H. Ohkawa, T. Hirano, S. Maki, H. Niwa, M. Oshashi, S. Inouye and F. I. Tsuji, *Tetrahedron Lett.*, 1998, **39**, 5239.
- J. Penalva, R. Vuchades, A. Maquieira, S. Gee and B. D. Hammock, *Biosens. Bioelectron.*, 2000, **15**, 99.
- K. Gottwald and D. Seebach, *Tetrahedron*, 1999, **55**, 723.
- T. L. Ho, *Carbocycle Construction in Terpene Synthesis*, Wiley-VCH, Weinheim, 1988.
- K. -I. Takao, R. Munakata and K. -I. Tadano, *Chem. Rev.*, 2005, **105**, 4779.
- M. E. Jung and D. G. Ho, *Org. Lett.*, 2007, **9**, 375.
- M. E. Krafft and T. F. N. Haxell, *J. Am. Chem. Soc.*, 2005, **127**, 10168.
- R. H. Grubbs, S. J. Miller and G. C. Fu, *Acc. Chem. Res.*, 1995, **28**, 446.
- H. Kim, S. D. Goble and C. Lee, *J. Am. Chem. Soc.*, 2007, **129**, 1030.
- D. Enders, M. R. M. Huttl, C. Grondal and G. Raabe, *Nature*, 2006, **441**, 861.
- Y. S. Tran and O. Kwon, *J. Am. Chem. Soc.*, 2007, **129**, 12632.
- M. Scholl, T. M. Trnka, J. P. Morgan and R. H. Grubbs, *Tetrahedron Lett.*, 1999, **40**, 2247.
- M. Scholl, S. Ding, C. W. Lee and R. H. Grubbs, *Org. Lett.*, 1999, **1**, 953.
- Q. Yang, H. Alper and W.-J. Xiao, *Org. Lett.*, 2007, **9**, 769.
- D. B. Berkowitz, J. M. McFadden and M. K. Sloss, *J. Org. Chem.*, 2000, **65**, 2907.
- S. E. Gibson, N. Guillo and M. J. Tozer, *Tetrahedron*, 1999, **55**, 585.
- K. N. Koch, A. Linden and H. Heimgartner, *Helv. Chim. Acta*, 2000, **83**, 233.
- J. R. Cronin and S. Pizzarello, *Science*, 1997, **275**, 951.
- T. Kan, Y. Kawamoto, T. Asakawa, T. Furuta and T. Fukuyama, *Org. Lett.*, 2008, **10**, 168.
- (a) E. Benedetti, B. Di Blasio, V. Pavone, C. Pedone and A. Santini, *Biopolymers*, 1989, **28**, 175; (b) P. K. C. Paul, M. Sukumar, R. Bardi, A. M. Piazzesi, G. Valle, C. Toniolo and P. Balaram, *J. Am. Chem. Soc.*, 1986, **108**, 6363.
- E. Erlenmeyer, *Annalen*, 1893, **275**, 1.
- P. A. Conway, K. Devine and F. Paradisi, *Tetrahedron*, 2009, **65**, 2935.
- H. Nakamura and K. J. Shimizu, *Tetrahedron Lett.*, 2011, **52**, 426.
- E. Yoshikawa, K. V. Radhakrishnan and Y. Yamamoto, *Tetrahedron Lett.*, 2000, **41**, 729.
- N. Solin, S. Narayan and K. J. Szabó, *J. Org. Chem.*, 2001, **66**, 1686.
- M. Jeganmohan, M. Shanmugasundaram and C.-H. Cheng, *Org. Lett.*, 2003, **5**, 881.
- J. A. Ibers, W. C. Hamilton, *International Tables for X-ray Crystallography*, Kynoch Press, Birmingham, 1974.



Contents lists available at ScienceDirect

International Journal of Pediatric Otorhinolaryngology

journal homepage: www.elsevier.com/locate/ijporlPrevalence of *GJB2* causing recessive profound non-syndromic deafness in Japanese childrenChieri Hayashi^{a,*}, Manabu Funayama^b, Yuanzhe Li^c, Kazusaku Kamiya^a, Atsushi Kawano^d, Mamoru Suzuki^d, Nobutaka Hattori^{b,c}, Katsuhisa Ikeda^a^a Department of Otorhinolaryngology, Juntendo University School of Medicine, 2-1-1 Hongo, Bunkyo-ku, Tokyo 113-8421, Japan^b Research Institute for Diseases of Old Age, Juntendo University School of Medicine, Japan^c Department of Neurology, Juntendo University School of Medicine, Japan^d Department of Otorhinolaryngology, Tokyo Medical University School of Medicine, Tokyo, Japan

ARTICLE INFO

Article history:

Received 14 June 2010

Received in revised form 18 October 2010

Accepted 2 November 2010

Available online 26 November 2010

Keywords:

Congenital deafness
Cochlear implantation
Japanese children
p.P225L
Connexin 26
GJB2

ABSTRACT

Objective: *GJB2* (gap junction protein, beta 2, 26 kDa; connexin 26) is a gap junction protein gene that has been implicated in many cases of autosomal recessive non-syndromic deafness. Point and deletion mutations in *GJB2* are the most frequent cause of non-syndromic deafness across racial groups. To clarify the relation between profound non-syndromic deafness and *GJB2* mutation in Japanese children, we performed genetic testing for *GJB2*.

Methods: We conducted mutation screening employing PCR and direct sequencing for *GJB2* in 126 children who had undergone cochlear implantation with congenital deafness.

Results: We detected 10 mutations, including two unreported mutations (p.R32S and p.P225L) in *GJB2*. We identified the highest-frequency mutation (c.235delC: 44.8%) and other nonsense or truncating mutations, as in previous studies. However, in our research, p.R143W, which is one of the missense mutations, may also show an important correlation with severe deafness.

Conclusion: Our results suggest that the frequencies of mutations in *GJB2* and *GJB6* deletions differ among cohorts. Thus, our report is an important study of *GJB2* in Japanese children with profound non-syndromic deafness.

© 2010 Elsevier Ireland Ltd. All rights reserved.

1. Introduction

People with any degree of sensory impairment may encounter problems such as discrimination within the education system or when looking for work, and a reduced life expectancy. Sensorineural hearing loss (SNHL) is the most common sensory impairment in developed societies [1,2], where one child in 1000 presents at birth with severe or profound deafness [3].

Recent advances in human genetics have indicated that more than half of congenital SNHL cases involve a genetic factor [4]. In 75–80% of genetic cases, SNHL is the result of autosomal recessive inheritance, and both parents have normal hearing [5]. Mutations of *GJB2* are the most frequent cause of autosomal recessive non-syndromic deafness. Indeed, previous studies have shown that *GJB2* mutations account for up to 50% of non-syndromic deafness cases [6]. Hearing-impaired subjects with biallelic *GJB2* mutations range widely but most commonly follow a severe to profound and non-progressive pattern [7–9]. About 100 different *GJB2* muta-

tions have been reported globally [the Connexin-Deafness homepage: <http://davinci.crg.es/deafness/>], and these mutations show a relatively high local dependence (founder effect). A high prevalence of c.35delG has been found among Caucasians; c.235delC among Eastern Asians, including Japanese [10–13]; c.167delT among Ashkenazi Jews [14]; p.R143W among certain Africans [15]; and p.W24X among Indians [16,17] and European Gypsies [18–20]. Some recent reports have indicated a genotype-phenotype correlation: children with two truncating mutations, such as c.35delG or c.235delC, are profoundly deaf, while children with a truncating and missense mutation, or two missense mutations, show better hearing [9,21,22]. Since improved speech performance after cochlear implantation in early childhood is usually observed in hearing-impaired subjects with *GJB2* mutations [23], the genetic testing of newborn babies will provide useful prognostic information when selecting appropriate treatment for such children.

In the present study, to clarify the frequency and genotype-phenotype correlation of *GJB2* mutations in children with profound non-syndromic deafness, we performed genetic testing for *GJB2* mutations involving 119 Japanese children who had undergone cochlear implantation with congenital deafness.

* Corresponding author. Tel.: +81 3 5802 1229; fax: +81 3 5840 7103.
E-mail address: chieri-h@juntendo.ac.jp (C. Hayashi).

2. Materials and methods

2.1. Subjects

We enrolled 119 Japanese children, who were unrelated to each other, with non-syndromic deafness for genetic analysis. Of these, 107 were sporadic cases (with only one affected individual in the family); the remaining 12 patients were autosomal recessive cases (with normal hearing parents and at least two affected children). The study sample consisted of 70 males (58.8%) and 49 females (41.2%). All of their hearing impairment levels were severe (71–95 dB) to profound (>95 dB); impairments were detected between 0 and 3 years old. All children had undergone cochlear implantation at Tokyo Medical University School of Medicine.

All cases underwent otoscopic examination and audiometric testing. Subjective tests of hearing acuity were assessed based on the auditory brain-stem response (ABR) and auditory steady-state response (ASSR) in infants and children. Behavioral observation audiometry (BOA) was used as a subsidiary measure to ABR and ASSR. A detailed history was taken to exclude other possible causes of deafness (such as neonatal complications, bacterial meningitis or other infections, use of ototoxic medication, or head trauma). Extended pedigrees were elicited from each family to exclude interfamilial relations. Temporal bone computed tomography was used in children to exclude any anomalies. The control group was carefully chosen to determine the carrier frequency, and consisted of 150 unrelated individuals with normal hearing.

Informed consent was obtained from the parents or guardians when necessary, and these were approved by the Ethical Committees of Juntendo University School of Medicine.

2.2. Genetic analysis

All samples from the children and normal controls were extracted from peripheral blood using the QIAamp DNA Blood Mini Kit (QIAGEN, Germantown, MD, USA). The coding region of *GJB2* was amplified from DNA samples by the polymerase chain reaction (PCR) using the primers *GJB2-F* 5'-GTGTGCATTCGCTTTTCCAG-3' and *GJB2-R* 5'-GCCACTGAGCCTTGACA-3'. PCR products were sequenced using the PCR primers and sequence primers *GJB2-A* 5'-CCACGCCAGCGCTCCTAGTG-3' and *GJB2-B* 5'-GAAGATGCTGCTGCTTGTGTAGG-3'. The sequencing reaction products were electrophoresed on an ABI Prism 310 Analyzer (Applied Biosystems). When no mutation or a single heterozygous mutation in *GJB2* was confirmed, we performed the multiplex PCR assay and direct sequencing for the coding region of *GJB6*. Multiplex PCR was carried out according to the method of Del Castillo et al. [24] to confirm the presence of the del(*GJB6*-D13S1830) and del(*GJB6*-D13S1854) deletions in *GJB6*.

Samples with no mutation or a single heterozygous mutation in *GJB2* and *GJB6* were analyzed for the gene dosage using real-time quantitative PCR (qPCR) to detect exon rearrangements in *GJB2* and *GJB6*. qPCR was performed with TaqMan Gene Expression Assays (Hs00269615_s1 for *GJB2*, and Hs00272726_s1 for *GJB6*, Applied Biosystems) and the 7500 Fast Real-Time PCR System (Applied Biosystems).

We obtained blood samples from the family which had one of two unreported mutations, pP225L, and the unreported one was confirmed as follows. The samples were subjected to mutation screening by PCR and direct sequencing for *GJB2*. The PCR product was subcloned into pCR 2.1 vecto-TOPO by TOPO TA cloning (Invitrogen, Carlsbad, CA, USA), and independent subclones were sequenced employing M13forward (5'-TTGTAACACGACGGCCAG) and reverse (5'-ACACAGGAAACAGCTATG) primers. The sequence data using in this study have been submitted to the GenBank

databases under accession numbers X65361, AB098335, NM_000816, and NM_001037.

2.3. Statistical analysis

A Z-test was used to calculate the difference in the allele frequency. In all statistical analyses, *P*-values of 0.01 or less were considered significant.

3. Results

3.1. Mutation screening of *GJB2*

GJB2 mutations were found in 45 of the 119 affected individuals, and, of these, 35 patients were homozygous or compound heterozygous (29.4%). *GJB2*-related deafness patients, who had two *GJB2* mutant alleles, were found in 7 of 12 familial cases (58.3%), and there were 28 of 107 sporadic cases (26.2%). Eight mutations, including two unreported ones (p.R32S and p.P225L), were identified in these patients (Table 1). Three mutations were truncating mutations [one was a nonsense mutation (p.Y136X), and two were frameshifts (c.235delC and c.176-191del)]. The remaining five were missense mutations (p.R143W, p.G45E, p.T86R, p.R32S, and p.P225L). Among these mutations, c.235delC was the most frequent. The c.235delC mutation accounted for 52.9% (37 of 70) of the *GJB2*-mutated alleles (Table 1).

We identified 10 subjects who had three or more mutations. All of them had p.G45E and p.Y136X, including one homozygous child. TA cloning and sequencing of subcloned PCR products revealed that all subjects had both mutations in the same allele (data not shown). G45E accompanied with Y136X has been reported as a pathogenic mutation in previous reports, especially in Japanese patients [11,25], although it remains unclear which mutation is more related to the pathogenicity.

We compared the allele frequency for each mutation with that in Ohtsuka's study [25] (Fig. 1). The frequency of c.235delC and three mutations (p.R143W, p.G45E/Y136X, and c.176-191del) in this study were significantly different from that in Ohtsuka's study (*P* < 0.01). While the p.V371 mutation was reported to be the second most frequent autosomal recessive deafness allele in Asian countries [11,12], the present subjects did not follow this pattern.

In one subject, we identified a missense mutation, p.P225L, which has not previously been reported (Fig. 2). The sister and father of the proband had this mutation, while they showed a normal hearing function. The mother, with a normal hearing function, showed no mutation at this site, while she revealed only heterozygous p.G45E/Y136X mutation as a known pathogenic mutation of *GJB2*. The sequencing results of TA cloning further confirmed the existence of the pP225L nonsense mutation in this patient. We also identified another unreported mutation, p.R32S, in another subject. The patient had p.R32S/p.G45E/Y136X mutations. The amino acid positions of two unreported mutations

Table 1

Mutations identified in the *Cx26* gene, *GJB2* (NG_008358.1), in child cases of congenital deafness.

Nucleotide change	Amino acid change	Allele (%)
c.235delC	p.Leu79CysfsX3	37 (52.9)
c.427C>T	p.Arg143Trp(p.R143W)	15 (21.4)
c.134G>A/c.408C>A	p.Gly45Glu/p.Tyr136X(p.G45E/Y136X)	10 (14.3)
c.176_191del	p.Gly59AlafsX18	4 (5.7)
c.257C>G	p.Thr86Arg(p.T86R)	2 (2.9)
c.94C>A	p.Arg32Ser ^a (p.R32S)	1 (1.4)
c.674C>T	p.Pro225Leu ^a (p.P225L)	1 (1.4)
Total mutations		70 (100)

^a Novel mutations detected in this study.

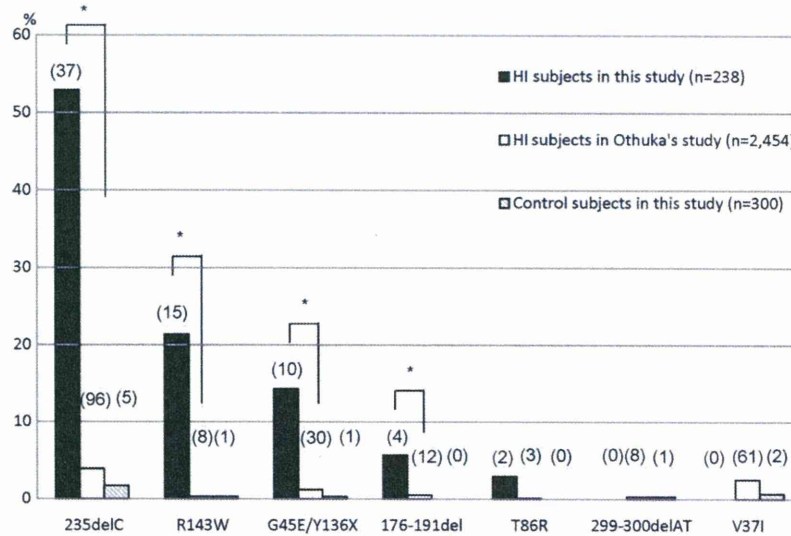


Fig. 1. Allele frequency for each mutation in three groups. A Z-test was used to assess the difference in frequency. Note the P-value of <0.01 between the two deafness groups for c.235delC, p.R143W, p.G45E/Y136X, and c.176-191del. *P < 0.01.

(p.R32S and p.P225L) are highly conserved among various species, and we did not detect any of these mutations in 300 chromosomes in normal Japanese controls.

4. Discussion

In this study, *GJB2*-related deafness patients accounted for 29.4% of non-syndromic deafness cases. This frequency was less than in a previous report, which pointed to a frequency of around 50% [6]. Familial cases were twice as prevalent as sporadic cases. In most of the previously reported studies, the prevalence of *GJB2* mutations was significantly higher in familial non-syndromic deafness than in sporadic cases [7,26,27]. The frequent mutations of *GJB2* (c.235delC, p.R143W, p. G45E/Y136X, and c.176-191del) in this study were partly different from previous reports [25]. It is assumed that all of our subjects had severe to profound deafness,

as they had received cochlear implants, whereas Ohtsuka's subjects had mild to profound deafness and included heterozygous mutations. A few studies have confirmed that some genotypes are correlated with clinical phenotypes in *GJB2*-related deafness. Further, truncating mutations are associated with a greater degree of deafness than non-truncating mutations [9,21,22]. For this reason, three of these cases might be truncating mutations. In contrast, p.R143W mutation was previously implicated in an extraordinarily high prevalence of profound deafness in Ghana [15,28] and Caucasians [9]. This missense mutation may also show an important correlation with severe deafness in Japan. On the other hand, an effect of geography on the allele frequency may have been present, because most of our subjects were from a different area compared to a previous report [25].

The relation between p.V37I mutation of *GJB2* and SNHL is controversial. While some reports suggest that this mutation is

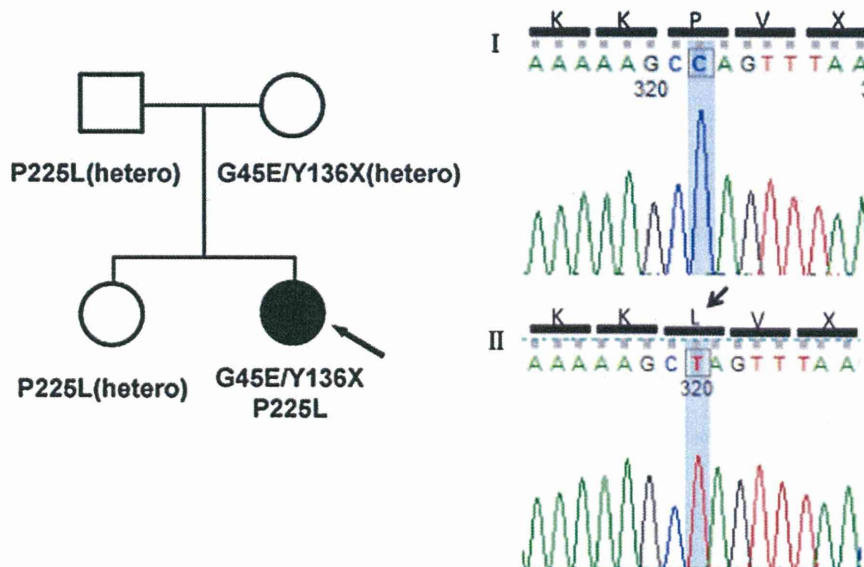


Fig. 2. (A) The pedigree and PCR direct sequencing results for the family; the arrow indicates the proband. (B) The sequencing results on TA cloning. Genomic PCR products were subcloned into a plasmid vector and sequenced separately (see Section 2). The sequences from independent clones are shown in the above two examples. I shows wild-type sequence, whereas II shows mutated sequence in which the proline residue is changed to leucine. Three of 8 subclones showed a missense mutation similar to that in II.

more common among individuals of Asian ancestry [11,12,29], others suggest that homozygous p.V371 is associated with slight/mild hearing loss [22,30,31]. In this study, no cases of homozygous p.V371 were observed. These findings support that this mutation is associated with mild hearing loss, because all of our subjects showed severe deafness.

The two unreported *GJB2* mutations, p.R32S and p.P225L, were not detected in normal hearing controls. These appeared in amino acid residues that were highly conserved. Additionally, three types of mutation were seen in arginine as the thirty-second amino acid, such as p.R32C, p.R32L, and p.R32H. Therefore, R32 is thought to be a mutation “hot spot.” Thus, it is likely that these are pathological mutations, rather than rare or functionally neutral polymorphic changes. On the other hand, the mutation site of p.P225 located at the C-terminus of Connexin26 has not previously been reported. As the C-terminus region of connexins is thought to be an important region for intracellular molecular signaling and interaction with scaffolding proteins and the cytoskeleton [32–34], p.P225L mutation found in this study may affect important intracellular molecular networks to maintain the normal function of the cochlear gap junction.

5. Conclusion

In conclusion, this study identified significant genotypic features of Japanese children with profound non-syndromic deafness. Further research is required covering a broader range of genes in the subjects in this study with either single heterozygous or no mutation, in order to better understand the epidemiology of deafness in Japan.

Acknowledgements

We thank all the subjects who participated in the present study. We also thank Ms. Naoko Tamura and Ms. Tomoko Kataoka (Tokyo Medical University School of Medicine), for recruiting families with non-syndromic deafness, and Ms. Junko Onoda (Juntendo University School of Medicine) for assisting in our experiments.

References

- [1] A.C. Davis, The prevalence of deafness and reported hearing disability among adults in Great Britain, *Int. J. Epidemiol.* 18 (1989) 911–917.
- [2] D.H. Wilson, P.G. Walsh, L. Sanchez, The epidemiology of deafness in an Australian adult population, *Int. J. Epidemiol.* 28 (1999) 247–252.
- [3] N.E. Morton, Genetic epidemiology of deafness, *Ann. N. Y. Acad. Sci.* 630 (1991) 1631.
- [4] M.L. Marazita, L.M. Ploughman, B. Rawlings, E. Remington, K.S. Arnos, W.E. Nance, Genetic epidemiological studies of early-onset deafness in the U.S. school-age population, *Am. J. Med. Genet.* 46 (1993) 486–491.
- [5] V. Kalatzis, C. Petit, The fundamental and medical impacts of recent progress in research on hereditary hearing loss, *Hum. Mol. Genet.* 7 (1998) 1589–1597.
- [6] A. Kenneson, K. Van Naarden Braun, C. Boyle, *GJB2* (connexin 26) variants and nonsyndromic sensorineural hearing loss: a HuGE review, *Genet. Med.* 4 (2002) 258–274.
- [7] F. Denoyelle, S. Marlin, D. Weil, L. Moatti, P. Chauvin, E.N. Garabedian, et al., Clinical features of the prevalent form of childhood deafness, *DFNB1*, due to a connexin-26 gene defect: Implications for genetic counselling, *Lancet* 353 (1999) 1298–1303.
- [8] A. Murgia, E. Orzan, R. Polli, M. Martella, C. Vinanzi, E. Leonardi, et al., Cx26 deafness: mutation analysis and clinical variability, *J. Med. Genet.* 36 (1999) 829–832.
- [9] R.L. Snoeckx, P.L. Huygen, D. Feldmann, S. Marlin, F. Denoyelle, J. Waligora, et al., *GJB2* mutations and degree of hearing loss: a multicenter study, *Am. J. Hum. Genet.* 77 (2005) 945–957.
- [10] Y. Fuse, K. Doi, T. Hasegawa, A. Sugii, H. Hibino, T. Kubo, Three novel connexin26 gene mutations in autosomal recessive non-syndromic deafness, *Neuro Report* 10 (1999) 1853–1857.
- [11] S. Abe, S. Usami, H. Shinkawa, P.M. Kelley, W.J. Kimberling, Prevalent connexin 26 gene (*GJB2*) mutations in Japanese, *J. Med. Genet.* 37 (2000) 41–43.
- [12] T. Kudo, K. Ikeda, S. Kure, Y. Matsubara, T. Oshima, K. Watanabe, et al., Novel mutations in the connexin 26 gene (*GJB2*) responsible for childhood deafness in the Japanese population, *Am. J. Med. Genet.* 90 (2000) 141–145.
- [13] H.J. Park, S.H. Hahn, Y.M. Chun, K. Park, H.N. Kim, Connexin 26 mutations associated with nonsyndromic hearing loss, *Laryngoscope* 110 (2000) 1535–1538.
- [14] P. Gasparini, R. Rabionet, G. Barbutani, S. Melchionda, M. Petersen, K. Brøndum-Nielsen, et al., High carrier frequency of the 35delG deafness mutation in European populations, Genetic Analysis Consortium of *GJB2* 35delG, *Eur. J. Hum. Genet.* 8 (2000) 19–23.
- [15] G.W. Brobby, B. Muller-Myhsok, R.D. Horstmann, Connexin 26 R143W mutation associated with recessive nonsyndromic sensorineural deafness in Africa, *N. Engl. J. Med.* 338 (1998) 548–550.
- [16] M. Maheshwari, R. Vijaya, M. Ghosh, S. Shastri, M. Kabra, P.S. Menon, Screening of families with autosomal recessive non-syndromic hearing impairment (ARNSHI) for mutations in *GJB2* gene: Indian scenario, *Am. J. Med. Genet. A* 120A (2003) 180–184.
- [17] M. RamShankar, S. Girirajan, O. Dagan, H.M. Ravi Shankar, R. Jalvi, R. Rangasayee, et al., Contribution of connexin26 (*GJB2*) mutations and founder effect to non-syndromic hearing loss in India, *J. Med. Genet.* 40 (2003) e68.
- [18] G. Minárik, V. Ferák, E. Feráková, A. Fieck, H. Poláková, L. Kádasi, High frequency of *GJB2* mutation W24X among Slovak Romany (Gypsies) patients with non-syndromic hearing loss (NSHL), *Gen. Physiol. Biophys.* 22 (2003) 549–556.
- [19] P. Seeman, M. Malíková, D. Rasková, O. Bendová, D. Groh, M. Kubálková, et al., Spectrum and frequencies of mutations in the *GJB2* (Cx26) gene among 156 Czech patients with pre-lingual deafness, *Clin. Genet.* 66 (2004) 152–157.
- [20] A. Alvarez, I. del Castillo, M. Villamar, L.A. Aguirre, A. González-Neira, A. López-Nevo, et al., High prevalence of the W24X mutation in the gene encoding connexin-26 (*GJB2*) in Spanish Romani (gypsies) with autosomal recessive non-syndromic hearing loss, *Am. J. Med. Genet. A* 137A (2005) 255–258.
- [21] K. Cryns, E. Orzan, A. Murgia, P.L. Huygen, F. Moreno, I. del Castillo, et al., A genotype-phenotype correlation for *GJB2* (connexin 26) deafness, *J. Med. Genet.* 41 (2004) 147–154.
- [22] T. Oguchi, A. Ohtsuka, S. Hashimoto, A. Oshima, S. Abe, Y. Kobayashi, et al., Clinical features of patients with *GJB2* (connexin 26) mutations: Severity of hearing loss is correlated with genotypes and protein expression patterns, *J. Hum. Genet.* 50 (2005) 76–83.
- [23] K. Fukushima, K. Sugata, N. Kasai, S. Fukuda, R. Nagayasu, N. Toida, et al., Better speech performance in cochlear implant patients with *GJB2*-related deafness, *Int. J. Pediatr. Otorhinolaryngol.* 62 (2002) 151–157.
- [24] F.J. Del Castillo, M. Rodríguez-Ballesteros, A. Alvarez, T. Hutchin, E. Leonardi, C.A. de Oliveira, et al., A novel deletion involving the connexin-30 gene, *del(GJB6-d13s1854)*, found in trans with mutations in the *GJB2* gene (connexin-26) in subjects with *DFNB1* non-syndromic deafness, *J. Med. Genet.* 42 (2005) 588–594.
- [25] A. Ohtsuka, I. Yuge, S. Kimura, A. Namba, S. Abe, L. Van Laer, et al., *GJB2* deafness gene shows a specific spectrum of mutations in Japan, including a frequent founder mutation, *Hum. Genet.* 112 (2003) 329–333.
- [26] J. Löffler, D. Nekahm, A. Hirst-Stadlmann, B. Gunther, H.J. Menzel, G. Utermann, et al., Sensorineural hearing loss and the incidence of Cx26 mutations in Austria, *Eur. J. Hum. Genet.* 9 (2001) 226–230.
- [27] A. Pampanos, J. Economides, V. Iliadou, P. Neou, P. Leotsakos, N. Voyiatzis, et al., Prevalence of *GJB2* mutations in prelingual deafness in the Greek population, *Int. J. Pediatr. Otorhinolaryngol.* 65 (2002) 101–108.
- [28] C. Hamelmann, G.K. Amedofu, K. Albrecht, B. Muntau, A. Gelhaus, G.W. Brobby, et al., Pattern of connexin 26 (*GJB2*) mutations causing sensorineural deafness in Ghana, *Hum. Mutat.* 18 (2001) 84–85.
- [29] WangYC, C.Y. Kung, M.C. Su, C.C. Su, H.M. Hsu, C.C. Tsai, et al., Mutations of Cx26 gene (*GJB2*) for prelingual deafness in Taiwan, *Eur. J. Hum. Genet.* 10 (2002) 495–498.
- [30] C. Huculak, H. Bruyere, T.N. Nelson, F.K. Kozak, S. Langlois, V371 connexin 26 allele in patients with sensorineural hearing loss: Evidence of its pathogenicity, *Am. J. Med. Genet. A* 140 (2006) 2394–2400.
- [31] H.H. Dahl, K. Saunders, T.M. Kelly, A.H. Osborn, S. Wilcox, B. Cone-Wesson, et al., Prevalence and nature of connexin 26 mutations in children with non-syndromic deafness, *Med. J. Aust.* 175 (2001) 191–194.
- [32] L.A. Elias, D.D. Wang, A.R. Kriegstein, Gap junction adhesion is necessary for radial migration in the neocortex, *Nature* 448 (2007) 901–907.
- [33] P.E. Martin, G. Blundell, S. Ahmad, R.J. Errington, W.H. Evans, Multiple pathways in the trafficking and assembly of connexin 26, 32 and 43 into gap junction intercellular communication channels, *J. Cell Sci.* 114 (2001) 3845–3855.
- [34] K.A. Schalper, N. Palacios-Prado, M.A. Retamal, K.F. Shoji, A.D. Martínez, J.C. Sáez, Connexin hemichannel composition determines the FGF-1-induced membrane permeability and free $[Ca^{2+}]_i$ responses, *Mol. Biol. Cell* 19 (2008) 3501–3513.